

EPR study of photoinduced reduction of nitroso compounds in titanium dioxide suspensions

Vlasta Brezová*, Peter Tarábek, Dana Dvoranová, Andrej Staško, Stanislav Biskupič

Department of Physical Chemistry, Faculty of Chemical and Food Technology, Slovak University of Technology in Bratislava, Radlinského 9, SK-812 37 Bratislava, Slovak Republic

Received 17 July 2002; received in revised form 21 August 2002; accepted 12 September 2002

Abstract

The radical intermediates produced upon UV irradiation of deoxygenated alcoholic titanium dioxide suspensions of nitrosobenzene, nitrobenzene, 2-nitrosotoluene, 2,3,5,6-tetramethylnitrosobenzene, 3,5-di-bromo-4-nitrosobenzenesulfonate (sodium salt), 2,4,6-tri-*t*-butyl-nitroso-benzene, and 2-methyl-2-nitrosopropane were investigated using in situ EPR technique. Nitrosobenzene is efficiently photoreduced in TiO₂ suspensions (toluene/alcohol, 1:1 (v/v)) forming exclusively one stable radical intermediate corresponding to C₆H₅N[•]OH species. The formation of this radical species is consistent with the proposed photocatalytic reduction mechanism, occurring from the primary generated nitrosobenzene mono-anion by the hydrogen abstraction from surroundings. The origin of hydrogen added to the nitroso group was demonstrated by the photocatalytic experiments using deuterated methanol, where the production of C₆H₅N[•]OD was established. Additionally, an identical radical C₆H₅N[•]OH was detected, when nitrobenzene was reduced under analogous experimental conditions. The photoinduced electron transfer from TiO₂ to nitroso compounds is accompanied by alcohol oxidation via the photogenerated titanium dioxide valance band holes forming alkoxy and hydroxyalkyl radicals. Production of hydroxyalkyl radicals ([•]CH₂OH, [•]CH(OH)CH₃, [•]C(OH)(CH₃)₂) with redox potentials suitable for a direct electron transfer to nitroso compounds represents an alternative reaction pathway for their reduction. On the other hand, the investigated nitroso derivatives are efficient spin-trapping agents, therefore, formation of nitroxyl radical spin adducts was observed in the photocatalytic experiments. The EPR spectra monitored upon irradiation of substituted nitrosobenzene derivatives in alcoholic TiO₂ suspensions reveal the correlation between nitrosobenzene derivative first step reduction potentials and yield of radical species produced.

© 2002 Elsevier Science B.V. All rights reserved.

Keywords: Nitroso compounds; Reduction; Hydroxyalkyl radicals; Spin-trapping agent; EPR, titanium dioxide; Photocatalysis

1. Introduction

In 1972, Fujishima and Honda [1] reported that water could be split into hydrogen and oxygen on a biased TiO₂ single-crystal electrode upon illumination. This observation has marked the beginning of an era of extensive research on semiconductor particles-based photovoltaic systems [2,3], photoelectrochemical conversion of solar to chemical energy [4–6], photocatalytic degradation of air and water pollutants [7–9], preparation of self-cleaning building materials [10], water and air disinfection [10], and photoelectrochemical methods for organic functional group transformation and metal recovery [11,12–15]. However, the destruction of a wide range of pollutants on semiconductor particles remains the most active area in semiconductor-mediated photocatal-

ysis research [7–9]. On the other hand, much less attention has been paid to the reductive transformations of organic compounds on semiconductor photocatalysts due to their redox properties, which are not as suitable for reductive transformations as for oxidative ones.

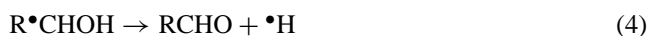
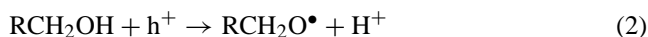
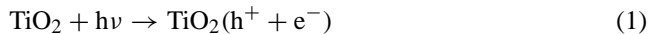
For a desired photoinduced electron transfer reaction to occur in semiconductor sensitized reactions, the relevant potential of the electron acceptor should be below (more positive than) the conduction band of the semiconductor, while the relevant potential of the electron donor is preferred to be above (more negative than) the valence band of the semiconductor [11]. Generally, a semiconductor-catalyzed reduction involves a series of electron transfer, protonation, and sometimes dehydration reactions [16]. Additionally, the hydrogen generated on the semiconductor reduction sites may also act as a reducing agent. An alcohol is usually used as a source of protons for the protonation, as well as an electron donor to suppress the electron–electron hole recombination [11]. When an alcohol is used as a solvent, it is oxidized during

* Corresponding author. Tel.: +421-7-529-26032;

fax: +421-7-524-93198.

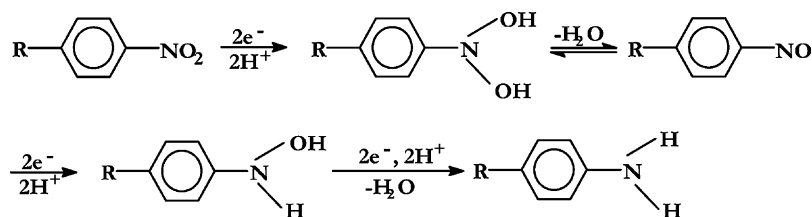
E-mail address: brezova@cvtstu.cvt.stuba.sk (V. Brezová).

irradiation by the photogenerated holes (h^+) to carbonyl compounds via alkoxy and hydroxyalkyl radical intermediates (Eqs. (1)–(3)). The hydrogen atom, which is being formed during reaction (Eq. (4)) may react with another one to form hydrogen molecule (Eq. (5)), or may be trapped by another molecule, which is then reduced. Since most of the organic substrates cannot compete with oxygen effectively (oxygen is a very good acceptor of a photoelectron), oxygen must be removed from the reaction system [11].

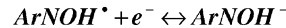
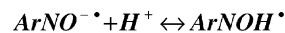
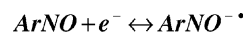


The reductive degradation of an organic compound is usually less efficient than an oxidative one. As a consequence, comparatively little research has been conducted on the fundamental nature of photocatalytic reduction. However, reductive processes may be more convenient for organic synthesis because they are functional group selective [11,17]. Compounds, which have been reduced photocatalytically include dioxygen [18], halogenated alkanes [19,20], chloroethylenes [21,22], viologens [23], and nitro compounds [11,16,24]. The photocatalytic multistep reduction of aromatic nitro compounds to amino derivatives on the irradiated TiO_2 photocatalysts was published formerly (Scheme 1) [16]. The selective photocatalytic reduction of 4-nitrophenol to 4-aminophenol in titanium dioxide suspensions prepared in different alcohols (methanol, ethanol, 1-propanol, 2-propanol, 1-butanol, *iso*-butanol) was investigated previously, and the results obtained demonstrated the significant influence of solvent characteristics (viscosity, polarity, polarisability) on the photoreduction yield [24].

Nitroso compounds are in every aspect very interesting and important substances. They constitute a chemical prototype with attractive potential pharmacological and toxicological properties [25–27]. Aromatic C-nitroso compounds can be formed as reactive intermediates in biological systems during metabolic pathways either by oxidation of arylamines or by reduction of aromatic nitro compounds, introduced into organism as a toxin [27–29]. Alternatively, some nitro compounds can enter into organisms as drugs,



Scheme 1. The reductive processes of aromatic nitro compounds in the irradiated TiO_2 suspensions [16].



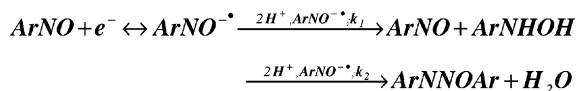
Scheme 2. Mechanism of aromatic nitroso compounds reduction in protic media [25,26,32].

and then they can be reduced to nitroso intermediates [30]. Consequently, the reduction properties of the nitroso group are of prime importance. The nitroso derivatives are also widely distributed in the environment and they can become carcinogenic, cytotoxic, and/or mutagenic after they enter into organism [25–29].

Some nitroso compounds are well known and in EPR spectroscopy often used spin-trapping agents [31]. Their usage is focused on the EPR investigation of short-lived radical intermediates, forming nitroxide adducts with characteristic hyperfine splittings. The main advantage of nitroso spin traps, in comparison with nitrones, lies in their ability of forming nitroxides, which give more direct information on the structure of the trapped radical [31]. The nitroso compounds may also exist as dimers, which dissociate in solutions to give monomers, and there is always the equilibrium between the monomeric and dimeric forms of the nitroso compounds in solution. For many nitroso spin traps, the monomer reduction potential is more positive than the dimer reduction potential [32].

Several studies have been done on electrochemical reduction of a group of nitroso derivatives in order to establish their redox properties (redox potentials), as well as to verify the presence of radicals in the reaction systems by virtue of in situ EPR techniques [25,26,32–34]. The oxidative and reductive behavior of several nitroso compounds has been characterized in aprotic media (*N,N*-dimethylformamide and acetonitrile), in order to evaluate their utility as spin traps in electrochemical processes [32–34]. The mechanism of aromatic nitroso compounds electrochemical reduction in protic and aprotic media was previously proposed (Schemes 2 and 3) [25,26,32].

Although some literature is available on photocatalytic reduction of nitro compounds [11,17,24], a comprehensive study dealing with photocatalytic reduction of nitroso compounds is still missing. Our paper is focused on the EPR study of radical intermediates formed upon irradiation of



Scheme 3. Mechanism of aromatic nitroso compounds reduction in aprotic media [25,26,32].

nitroso compounds in various alcoholic titanium dioxide suspensions in an effort to investigate the photocatalytic reduction of nitroso compounds with different structure.

2. Experimental details

2.1. Chemicals

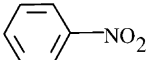
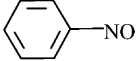
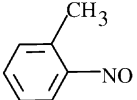
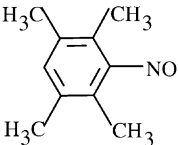
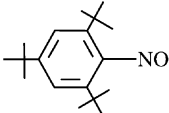
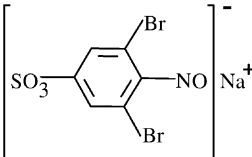
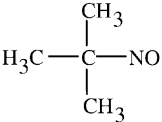
Titanium dioxide P25 high surface (Degussa, Germany) was used in all photocatalytic experiments in two concentrations: 0.1 and 1 g dm⁻³. Degussa P25 (high surface) is a non-porous anatase-rutile mixture with specific area of 75 m² g⁻¹. The solvents used, methanol (MeOH), ethanol (EtOH), toluene were purchased in spectroscopic grade from Lachema (Czech Republic), acetonitrile (ACN) from Fluka,

and 2-propanol (2-PrOH) GR dried from Merck (Germany). Deuterated methanol CD₃OD was obtained from Aldrich. Investigated nitroso and nitro compounds are summarized in Table 1. Redistilled water was used for the preparation of DBNBS solutions.

2.2. Techniques

The suspensions of TiO₂ were prepared in two concentrations: 0.2 and 2 g dm⁻³ in three various alcohols: methanol, ethanol and 2-propanol. All suspensions were sonicated for 30 s in an ultrasonic bath. The TiO₂ slurry was mixed with solution of nitroso or nitro compound in adequate solvent, i.e. toluene, water or acetonitrile, immediately prior to irradiation. In addition, we had prepared “blanks” without TiO₂ photocatalyst as well. The solutions or suspensions were carefully deoxygenated by a stream of argon, subsequently filled in the quartz flat cell optimized for the Bruker TM cylindrical EPR cavity. The X-band EPR spectra were recorded in situ using a field-modulated CW Bruker ER 200 D SRC EPR spectrometer, coupled with an Aspect 2000 computer, in the original single TM-110 (ER 4103 TM) cylindrical cavity. The high-frequency modulation (100 kHz)

Table 1
List of nitroso and nitro compounds used in experiments

Name of compound and abbreviation	Structural formula	Notes
Nitrobenzene (NO ₂ B)		Lachema (Czech Republic)
Nitrosobenzene (NOB)		Fluka
2-Nitrosotoluene (2-NOT)		Aldrich
2,3,5,6-Tetramethylnitrosobenzene (nitrosodurene) (ND)		Aldrich
2,4,6-Tri- <i>t</i> -butylnitroso-benzene ((<i>t</i> -Bu) ₃ NOB)		Sigma Chemical (USA)
3,5-Di-bromo-4-nitrosobenzenesulfonic acid (sodium salt) (DBNBS)		Sigma Chemical (USA)
2-Methyl-2-nitrosopropane (MNP)		Sigma Chemical (USA) (dimer)

was performed using two Helmholtz coils mounted into the left and right side walls of the cavity.

The samples were irradiated directly in the cavity of EPR spectrometer by HPA 400/30S lamp (Philips), which represents a medium-pressure metal halide source with iron and cobalt additives emitting ozone-free radiation mainly between 300 and 400 nm [35]. The lamp irradiance in UV/A region of 30 mW cm^{-2} inside the EPR cavity was calculated by a Compact radiometer UVPS (UV Process Supply Inc., USA). The radiation with wavelengths $\lambda > 300 \text{ nm}$ was selected by a Pyrex filter. The standard EPR experiments were performed at 290 K. Typical settings for the series of EPR experiments were as follows: center field 349 mT; sweep width 6–10 mT; gain $5 \times 10^4 - 2.5 \times 10^5$; modulation amplitude 0.025–0.1 mT; microwave power 20 mW; time constant 200 ms; sweep time 50 or 100 s. The *g*-factors were quoted with uncertainty of ± 0.0001 using an internal reference standard marker containing 1,1-diphenyl-2-picrylhydrazyl (DPPH) built into the EPR spectrometer. The simulations of the individual components of the EPR spectra were obtained using the commercially available *WinEPR* and *SimFonia* programs distributed by Bruker [36]. The complex experimental EPR spectra were then fitted as the linear combinations of these individual simulations using a least-squares minimization procedure with the *Scientist Program* (MicroMath). The statistical parameters of calculation procedure (R^2 , coefficient of determination and correlation) serve for the determination of simulation quality, i.e. harmonization of experimental and simulated spectra. The relative concentrations of the spin adducts were calculated from the contributions of the individual spectra to experimental spectrum.

UV-Vis spectra were recorded under argon using diode array UV-Vis spectrometer PC 1000 (Ocean Optics).

3. Results and discussion

3.1. Titanium dioxide mediated photoreductions

Fig. 1 and Table 2 summarize literature data for band-edge positions of TiO_2 measured versus SCE in acetonitrile solvent [37] and the potentials of the first reduction step of

Table 2

First step reduction potentials of investigated systems in acetonitrile solvent recalculated for SCE reference electrode along with the band-edge positions of titanium dioxide in acetonitrile vs. SCE [32,37]

Compounds	E_{p1} (V) (monomer)
NOB	−0.949
2-NOT	−1.039
ND	−1.179
(<i>t</i> -Bu) ₃ NOB	−1.259
DBNBS	Not available
MNP	−1.769
Band-edge positions of TiO_2 (V)	Conduction band Valence band
	−1.25 2.2

several monomeric forms of nitroso compounds [32]. The originally published values of reduction potentials obtained in ACN/0.1 M NEt_4ClO_4 versus Ag/AgNO_3 (0.01 M) ACN electrochemical systems were recalculated for SCE reference electrode [38]. The redox potentials are approximated from the values quoted for acetonitrile, as corresponding values for toluene/alcohols mixed solvent are not available thus far.

The driving force (ΔE) of the photochemical heterogeneous electron transfer from TiO_2 conduction band to the electron accepting nitroso compounds can be expressed using the following equation [16]:

$$\Delta E = E_{\text{cb}} - E_{\text{RNO/RNO}^{\bullet-}} \quad (6)$$

At this point, the highest driving force was calculated for nitrosobenzene (Table 2, Fig. 1). On the other hand, the alkyl substitution on nitrosobenzene molecule causes the reduction potential shift to more negative values [32], and consequently the driving force is reduced for 2-nitrosotoluene, nitrosodurene and 2,4,6-tri-*t*-butylnitrosobenzene. Theoretically, 2-methyl-2-nitrosopropane is due to the first reduction potential value of -1.77 V versus SCE unsuitable for the direct electron transfer, from TiO_2 conduction band, however, the electron injection to the photoexcited MNP molecule cannot be excluded. It should be noted here that under given experimental conditions the application of different solvent systems (toluene/alcohols) could result in the shift of corresponding potentials values enabling the photoelectron transfer to the nitroso compounds. No information on the reduction potentials of DBNBS in water/alcohol solvent was found in literature.

3.2. Reduction of nitrosobenzene and nitrobenzene in TiO_2 suspensions

In accordance with the earlier discussed mechanisms of photocatalytic reduction of nitroso and nitro compounds in alcoholic suspensions of titanium dioxide (Schemes 1–3), we propose that the primary photoinduced process represents electron transfer to nitrosobenzene molecule generating the corresponding mono-anion radical $\text{NOB}^{\bullet-}$, because the reduction potential of the nitrosobenzene first reduction step is appropriately positioned for the transfer of photogenerated TiO_2 conduction band electrons (Fig. 1 and Table 2). Simultaneously, methanol, ethanol and 2-propanol solvents are efficiently oxidized by TiO_2 valence holes forming hydroxymethyl, 1-hydroxyethyl and 2-hydroxypropyl radicals [11,17], which possess suitable reduction potentials [39] for the alternative pathway of nitrosobenzene reduction.

However, simulations of experimental EPR spectra measured upon continuous irradiation of NOB ($c_{\text{NOB}} = 1.5 \text{ mmol dm}^{-3}$, $\rho_{\text{TiO}_2} = 1 \text{ g dm}^{-3}$) in the toluene/MeOH, toluene/EtOH and toluene/2-PrOH (1:1 (v/v)) show merely the EPR signals characteristic for the addition of hydrogen atom to nitroso group, which result in the formation of $\text{C}_6\text{H}_5\text{N}^{\bullet}\text{OH}$ nitroxyl radical (Fig. 2). The parameters

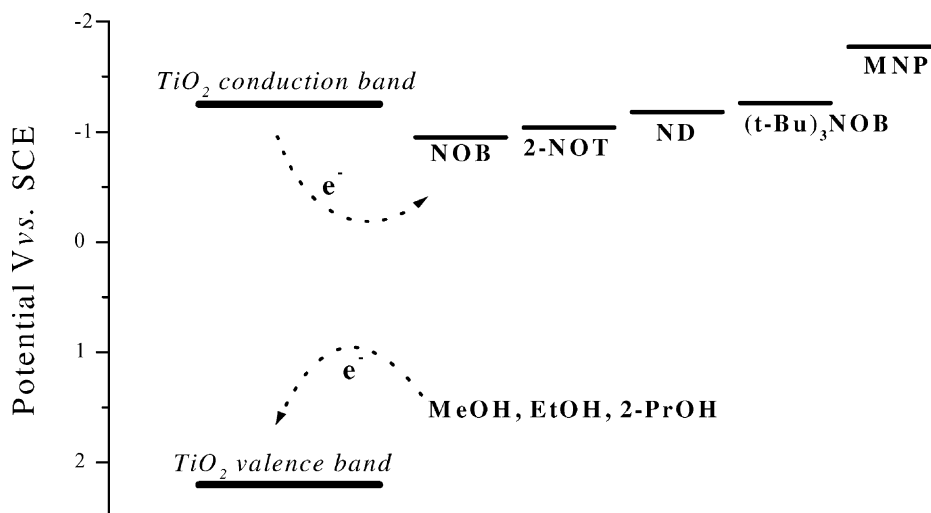


Fig. 1. Band-edge positions of titanium dioxide [37] and first step reduction potentials of investigated nitroso compounds [32] in acetonitrile solvent.

of the simulated EPR spectra are summarized in Table 3. Consequently, nitrosobenzene mono-anion, described in literature as sufficiently stable in aprotic solvents [25], rapidly converts under the given experimental conditions to $C_6H_5N^{\bullet}OH$ radical by proton abstraction from surround-

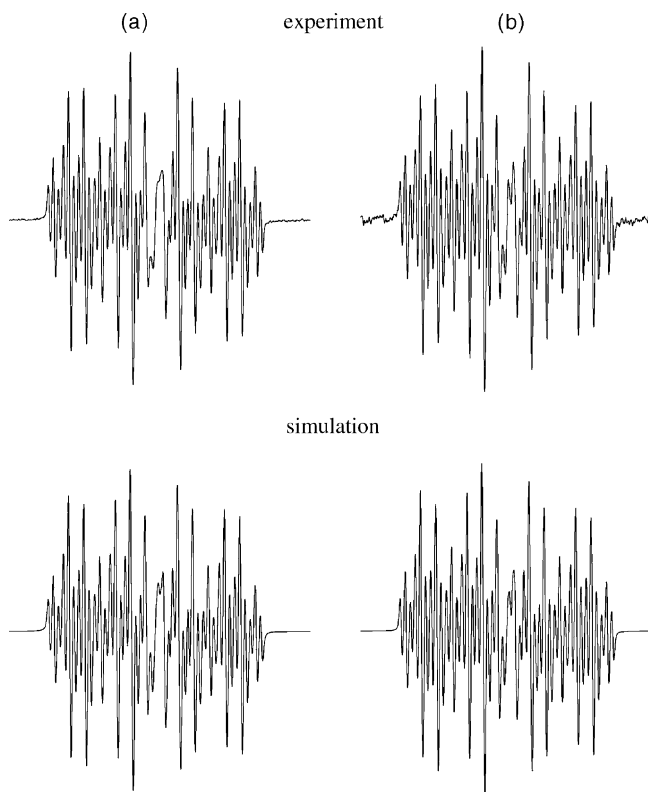


Fig. 2. Experimental and simulated EPR spectra (6 mT scan) obtained upon continuous irradiation of NOB in TiO_2 suspensions ($c_{NOB} = 1.5 \text{ mmol dm}^{-3}$, $\rho_{TiO_2} = 1 \text{ g dm}^{-3}$) deoxygenated by argon: (a) toluene/MeOH (1:1 (v/v)); (b) toluene/EtOH (1:1 (v/v)). The EPR parameters of simulated radical species are summarized in Table 3.

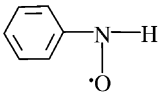
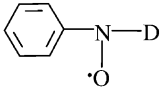
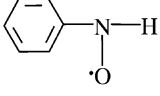
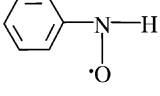
ings. Analogous EPR spectra of decreased intensity were monitored, when suspensions with lower TiO_2 concentration ($\rho_{TiO_2} = 0.1 \text{ g dm}^{-3}$) were irradiated. The role of titanium dioxide in the photocatalytic nitrosobenzene reduction was verified in blank photochemical experiments in which NOB was irradiated in titanium dioxide-free solutions of toluene/MeOH, toluene/EtOH and toluene/2-PrOH, and where only negligible intensity of EPR signals was observed.

The proton availability characterizes one of the significant factors of the nitro and nitroso derivatives photocatalytic reduction [11,16,17]. In an effort to determine the origin of hydrogen in the photogenerated $C_6H_5N^{\bullet}OH$ radical, we carried out photocatalytic reduction of NOB in TiO_2 suspensions prepared in CD_3OD . The EPR spectra observed upon continuous irradiation of nitrosobenzene in titanium dioxide suspensions in deuterated methanol ($c_{NOB} = 1.5 \text{ mmol dm}^{-3}$, $\rho_{TiO_2} = 1 \text{ g dm}^{-3}$, toluene/ CD_3OD 1:1 (v/v)) clearly confirm the presence of $C_6H_5N^{\bullet}OD$ radical species (Fig. 3, Table 3).

Nitrosobenzene molecule represents an effective spin-trapping agent of organic radicals [31]. However, in the experimental EPR spectra measured upon irradiation of NOB in titanium dioxide suspensions ($c_{NOB} = 1.5 \text{ mmol dm}^{-3}$, $\rho_{TiO_2} = 1$ or 0.1 g dm^{-3}) prepared in mixed solvents toluene/MeOH, toluene/ CD_3OD , toluene/EtOH, toluene/2-PrOH (1:1 (v/v)), no nitrosobenzene spin trap adducts with organic radicals are observed. The photogenerated radical species $\bullet CH_2OH$, $\bullet CD_2OD$, $CH_3\bullet CHO$, $(CH_3)_2\bullet COH$ are, due to their suitable positioned reduction potentials [39], efficiently incorporated in the electron transfer to nitrosobenzene molecule, and consequently, the unfavorable spin-trapping reaction pathway is suppressed. Generally, two reaction pathways can be postulated for these photogenerated radicals species, i.e. they may undergo efficient electron transfer reducing the nitroso compounds

Table 3

EPR parameters of radical species formed upon continuous irradiation of nitrosobenzene in titanium dioxide suspensions ($c_{\text{NOB}} = 1.5 \text{ mmol dm}^{-3}$, $\rho_{\text{TiO}_2} = 1 \text{ g dm}^{-3}$)

Solvent system	Radical	Splitting constants (mT)	g-Factor	Reference
Toluene/CH ₃ OH ^a		$a_{\text{N}}(\text{NO}) = 0.976$ $a_{\text{H}}(\text{NOH}) = 1.256$ $a_{\text{H}}(2\text{H}^o) = 0.307$ $a_{\text{H}}(2\text{H}^m) = 0.104$ $a_{\text{H}}(1\text{H}^p) = 0.331$	2.0055	[40,41]
Toluene/CD ₃ OD		$a_{\text{N}}(\text{NO}) = 0.959$ $a_{\text{D}}(\text{NOD}) = 0.192$ $a_{\text{H}}(2\text{H}^o) = 0.311$ $a_{\text{H}}(2\text{H}^m) = 0.105$ $a_{\text{H}}(1\text{H}^p) = 0.330$	2.0055	
Toluene/EtOH		$a_{\text{N}}(\text{NO}) = 0.972$ $a_{\text{H}}(\text{NOH}) = 1.253$ $a_{\text{H}}(2\text{H}^o) = 0.306$ $a_{\text{H}}(2\text{H}^m) = 0.105$ $a_{\text{H}}(1\text{H}^p) = 0.332$		
Toluene/2-PrOH		$a_{\text{N}}(\text{NO}) = 0.960$ $a_{\text{H}}(\text{NOH}) = 1.248$ $a_{\text{H}}(1\text{H}^o) = 0.297$ $a_{\text{H}}(1\text{H}^o) = 0.309$ $a_{\text{H}}(2\text{H}^m) = 0.103$ $a_{\text{H}}(1\text{H}^p) = 0.328$		

^a (1:1 (v/v)).

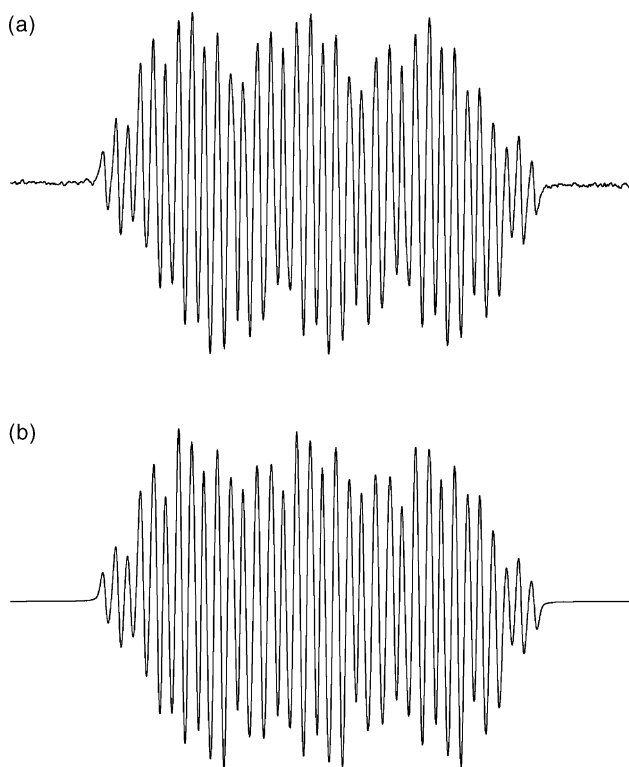
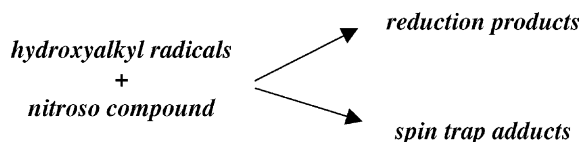


Fig. 3. Experimental (a) and simulated (b) EPR spectra (5 mT scan) obtained upon continuous irradiation of NOB in toluene/CD₃OD (1:1 (v/v)) TiO₂ suspensions ($c_{\text{NOB}} = 1.5 \text{ mmol dm}^{-3}$, $\rho_{\text{TiO}_2} = 1 \text{ g dm}^{-3}$) deoxygenated by argon. The EPR parameters of simulated radical species are summarized in Table 3.

by the alternative reduction mechanisms, or they may add to the nitroso group forming the corresponding paramagnetic nitroxyl spin adducts (Scheme 4). The ratio reduction/addition is significantly predisposed by the nitroso compounds first step reduction potentials.

The reductive process of aromatic nitrocompounds photosensitized by titanium dioxide results in the intermediate formation of nitroso derivatives (Scheme 1). Indeed, the EPR spectra measured upon irradiation of nitrobenzene in TiO₂ suspensions (toluene/MeOH, toluene/EtOH, toluene/2-PrOH; 1:1 (v/v)) establish formation of the C₆H₅N[•]OH radical, which is identical to the radical reduction product observed for nitrosobenzene (Fig. 4). On the other hand, generation of sufficient high concentration of C₆H₅N[•]OH species requires higher concentrations of nitrobenzene in the irradiated TiO₂ suspensions, and best results are obtained when $c_{\text{NO}_2\text{B}} = 80 \text{ mmol dm}^{-3}$. In order to stabilize the photogenerated anion-radicals formed by photocatalytic reduction of nitrobenzene, we have performed also the irradiation in acetonitrile/methanol TiO₂ suspensions replacing toluene by the more polar acetonitrile.



Scheme 4. Possible reaction pathways of photogenerated hydroxyalkyl radicals in investigated systems.

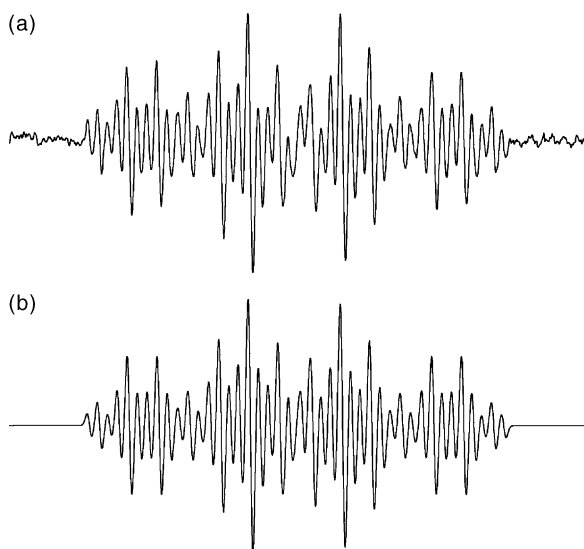


Fig. 4. Experimental (a) and simulated (b) EPR spectra (6 mT scan) obtained upon continuous irradiation of NO₂B in acetonitrile/MeOH (1:1 (v/v)) TiO₂ suspensions ($c_{\text{NO}_2\text{B}} = 80 \text{ mmol dm}^{-3}$, $\rho_{\text{TiO}_2} = 1 \text{ g dm}^{-3}$) deoxygenated by argon. The EPR parameters of simulated radical species are summarized in Table 4.

The EPR parameters of C₆H₅N•OH radical species summarized in Tables 3 and 4 show a slight growth of hyperfine splitting constants $a_{\text{N}}(\text{NO})$ and $a_{\text{H}}(\text{NOH})$ when the relative permittivity of the mixed solvents increases.

3.3. Reduction of 2-nitrosotoluene in TiO₂ suspensions

Núñez-Vergara et al. have investigated the electrochemical reduction of 2-NOT and 3-NOT to the corresponding mono-anion radicals in acetonitrile solvent by EPR spectroscopy [26]. The chemical step in the reduction of nitrosotoluene derivatives in acetonitrile corresponds to a dimerization of electrochemically generated mono-anions with the consecutive elimination of water, and presumably through participation of protons from the solvent to produce the azoxyderivatives (Scheme 3) [25,26]. The NMR investigations of the solvent induced effects on nitrogen shielding of nitrosobenzene derivatives showed the significant formation of dimeric isodioxy form of 2-NOT in 0.2 M solutions at 35 °C [42]. Azoxybenzene generation has been reported previously during the electrochemical reduction of NOB in acetonitrile [25], and similar behavior was observed also for 2-nitrosotoluene [26].

The mutual energetic positions of titanium dioxide conduction band photoelectrons and 2-nitrosotoluene first reduction step potential (Fig. 1, Table 2) allow effective photoinduced electron transfer to 2-NOT molecule upon irradiation of 2-NOT in TiO₂ alcoholic slurries. Despite of the complexity of the experimental EPR spectra measured during the continuous irradiation of 2-NOT in toluene/MeOH (1:1 (v/v)) TiO₂ suspensions ($c_{\text{NOT}} = 1.5 \text{ mmol dm}^{-3}$, $\rho_{\text{TiO}_2} = 0.1 \text{ g dm}^{-3}$), the simulations reveal the presence

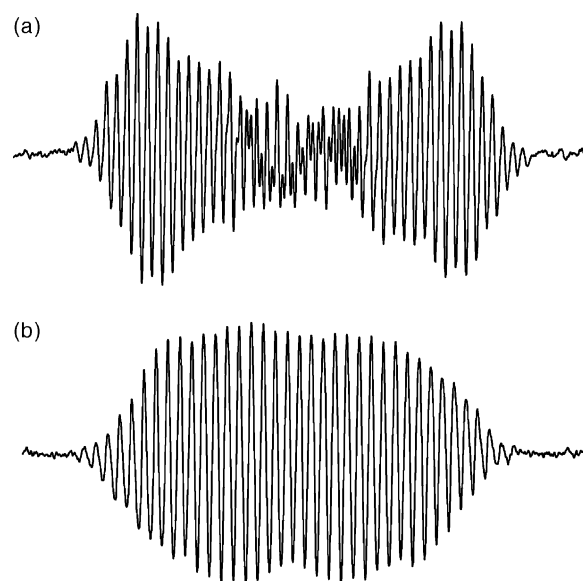


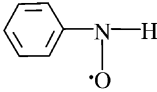
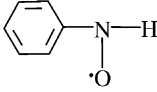
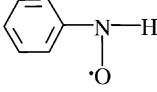
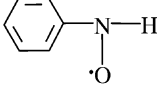
Fig. 5. EPR spectra measured upon continuous irradiation of 2-NOT in TiO₂ suspensions ($c_{\text{NOT}} = 1.5 \text{ mmol dm}^{-3}$, $\rho_{\text{TiO}_2} = 0.1 \text{ g dm}^{-3}$) deoxygenated by argon: (a) toluene/MeOH (1:1 (v/v)); 7 mT scan; (b) toluene/CD₃OD (1:1 (v/v)); 5 mT scan.

of at least two individual radical species (Fig. 5a). Our interpretation of experimental EPR spectra observed upon photocatalytic reduction of 2-NOT in toluene/alcohol TiO₂ suspensions is based on the presence of mono-anion radical (2-NOT)^{•-} and the (*o*-CH₃)C₆H₄N•OH nitroxyl radical. The parameters employed in the experimental EPR spectra simulations are summarized in Table 5. The splitting constant assignments used in our simulations of (2-NOT)^{•-} are in a good agreement with the hyperfine splittings determined by Núñez-Vergara et al. [26]. However, the statistical parameters of mathematical simulations demonstrate that improved harmony of experimental and simulated EPR spectra requires the incorporation of further radical species in the simulations. Consequently, we propose that during photocatalytic reduction of 2-NOT in toluene/alcohol titanium dioxide suspensions, the photogenerated hydroxyalkyl radicals are added to 2-NOT forming the corresponding spin adducts, but due to the complexity of the central part of the experimental EPR spectra, their hyperfine splittings were determined only ambiguously.

The presence of titanium dioxide photocatalyst is substantial for the efficient photoreduction of 2-NOT, as clearly shown by the results of blank experiments in which 2-nitrosotoluene has been irradiated in TiO₂-free solutions. The intensity of EPR signals monitored upon continuous irradiation of 2-NOT in toluene/alcohol TiO₂ suspensions sensitively reflects the concentration of titanium dioxide in the experimental systems. It should be noted here that the application of lower photocatalyst concentration ($\rho_{\text{TiO}_2} = 0.1 \text{ g dm}^{-3}$) results in the higher intensity of EPR signal as a consequence of a higher radical species concentration. At

Table 4

EPR parameters of radical species formed upon continuous irradiation of nitrobenzene in titanium dioxide suspensions ($c_{\text{NO}_2\text{B}} = 80 \text{ mmol dm}^{-3}$, $\rho_{\text{TiO}_2} = 1 \text{ g dm}^{-3}$)

Solvent system	Radical	Splitting constants (mT)	g-Factor	Reference
Toluene/CH ₃ OH ^a		$a_{\text{N}}(\text{NO}) = 0.973$ $a_{\text{H}}(\text{NOH}) = 1.258$ $a_{\text{H}}(2\text{H}^o) = 0.315$ $a_{\text{H}}(2\text{H}^m) = 0.105$ $a_{\text{H}}(1\text{H}^p) = 0.320$	2.0055	[40,41]
Toluene/EtOH		$a_{\text{N}}(\text{NO}) = 0.965$ $a_{\text{H}}(\text{NOH}) = 1.266$ $a_{\text{H}}(2\text{H}^o) = 0.313$ $a_{\text{H}}(2\text{H}^m) = 0.105$ $a_{\text{H}}(1\text{H}^p) = 0.315$		
Toluene/2-PrOH		$a_{\text{N}}(\text{NO}) = 0.958$ $a_{\text{H}}(\text{NOH}) = 1.254$ $a_{\text{H}}(2\text{H}^o) = 0.310$ $a_{\text{H}}(2\text{H}^m) = 0.104$ $a_{\text{H}}(1\text{H}^p) = 0.315$		
ACN/MeOH		$a_{\text{N}}(\text{NO}) = 0.960$ $a_{\text{H}}(\text{NOH}) = 1.255$ $a_{\text{H}}(2\text{H}^o) = 0.311$ $a_{\text{H}}(2\text{H}^m) = 0.105$ $a_{\text{H}}(1\text{H}^p) = 0.311$		

^a (1:1 (v/v)).

higher TiO₂ concentration the result may be in accord with the more effective incorporation of radical intermediates in the consecutive reactions forming the final diamagnetic photoreduction products.

Additionally, the experiments using deuterated methanol were performed, in which the EPR spectra were monitored during continuous irradiation of 2-NOT in titanium dioxide suspension ($c_{\text{NOT}} = 1.5 \text{ mmol dm}^{-3}$, $\rho_{\text{TiO}_2} = 0.1 \text{ g dm}^{-3}$) prepared in toluene/CD₃OD (1:1 (v/v)). Simulation analysis of the experimental EPR spectra confirms deuterium atom abstraction from deuterated methanol forming the nitroxyl radical, (*o*-CH₃)C₆H₄N[•]OD, with the characteristic deuterium splitting, and further paramagnetic species being indicative of 2-nitrosotoluene mono-anion radical formation (Fig. 5b, Table 5).

3.4. Reduction of nitrosodurene in TiO₂ suspensions

The significant cathodic shift in the reduction potentials of nitrosodurene (2,3,5,6-tetramethylnitrosobenzene) reflects mainly the inductive effect associated with the tetra alkylsubstitution [32]. The energy positions of TiO₂ conduction band-edge and the first reduction potential of ND in acetonitrile are suitable for photoinduced electron transfer to ND, forming the corresponding ND^{•-} mono-anion radical (Fig. 1, Table 2), although the driving force of photoinduced reduction process is significantly lower comparing to NOB or to 2-NOT. The decreased efficiency of nitrosodurene photocatalytic reduction in TiO₂ suspensions requires that nitrosodurene molecule behaves either as an electron acceptor or as a free radical scavenger, i.e. spin-trapping agent.

The application of EPR spin-trapping technique with the nitrosodurene spin trap yielded considerable information on the radical intermediates formation during thermally and photochemically induced reactions [31].

The electronic absorption spectrum of nitrosodurene in toluene shown in Fig. 6 shows the presence of absorption maxima at 300 and 322 nm, therefore, the direct excitation of ND under given experimental conditions cannot be excluded. Upon in situ irradiation of ND in toluene solutions ($c_{\text{ND}} = 1.5 \text{ mmol dm}^{-3}$) in blank experiments, we have observed

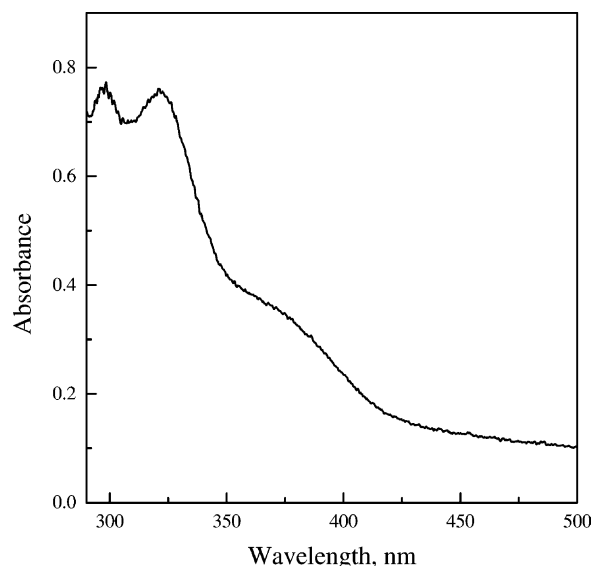
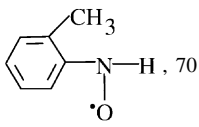
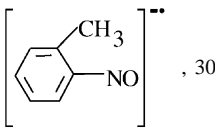
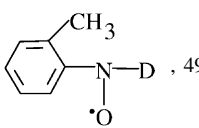
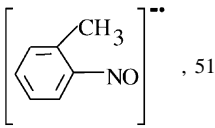
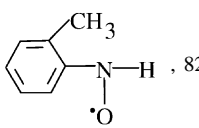
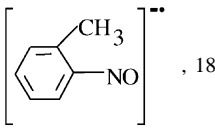
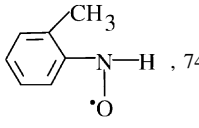
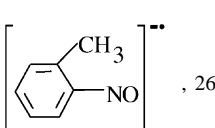


Fig. 6. UV-Vis absorption spectrum of nitrosodurene in toluene solvent ($c_{\text{ND}} = 75 \mu\text{mol dm}^{-3}$, cell length 1 cm).

Table 5

EPR parameters of radical species formed upon continuous irradiation of 2-nitrosotoluene in titanium dioxide suspensions ($c_{\text{NOT}} = 1.5 \text{ mmol dm}^{-3}$, $\rho_{\text{TiO}_2} = 0.1 \text{ g dm}^{-3}$)

Solvent system	Radical, relative concentration (%)	Splitting constants (mT)	g-Factor	Reference
Toluene/CH ₃ OH ^a	 , 70	$a_{\text{N}}(\text{NO}) = 1.079$ $a_{\text{H}}(\text{NOH}) = 1.130$ $a_{\text{H}}(3\text{H}^{\text{methyl}}) = 0.213$ $a_{\text{H}}(1\text{H}^{\text{o}}) = 0.213$ $a_{\text{H}}(2\text{H}^{\text{m}}) = 0.108$ $a_{\text{H}}(1\text{H}^{\text{p}}) = 0.324$	2.0055	
	 , 30	$a_{\text{N}}(\text{NO}) = 0.840$ $a_{\text{H}}(3\text{H}^{\text{methyl}}) = 0.213$ $a_{\text{H}}(1\text{H}^{\text{o}}) = 0.213$ $a_{\text{H}}(2\text{H}^{\text{m}}) = 0.104$ $a_{\text{H}}(1\text{H}^{\text{p}}) = 0.315$		2.0052
Toluene/CD ₃ OD	 , 49	$a_{\text{N}}(\text{NO}) = 1.063$ $a_{\text{D}}(\text{NOD}) = 0.195$ $a_{\text{H}}(3\text{H}^{\text{methyl}}) = 0.213$ $a_{\text{H}}(1\text{H}^{\text{o}}) = 0.213$ $a_{\text{H}}(2\text{H}^{\text{m}}) = 0.104$ $a_{\text{H}}(1\text{H}^{\text{p}}) = 0.315$	2.0055	
	 , 51	$a_{\text{N}}(\text{NO}) = 0.840$ $a_{\text{H}}(3\text{H}^{\text{methyl}}) = 0.213$ $a_{\text{H}}(1\text{H}^{\text{o}}) = 0.213$ $a_{\text{H}}(2\text{H}^{\text{m}}) = 0.102$ $a_{\text{H}}(1\text{H}^{\text{p}}) = 0.313$		
Toluene/EtOH	 , 82	$a_{\text{N}}(\text{NO}) = 1.078$ $a_{\text{H}}(\text{NOH}) = 1.127$ $a_{\text{H}}(3\text{H}^{\text{methyl}}) = 0.212$ $a_{\text{H}}(1\text{H}^{\text{o}}) = 0.212$ $a_{\text{H}}(2\text{H}^{\text{m}}) = 0.106$ $a_{\text{H}}(1\text{H}^{\text{p}}) = 0.325$		
	 , 18	$a_{\text{N}}(\text{NO}) = 0.830$ $a_{\text{H}}(3\text{H}^{\text{methyl}}) = 0.212$ $a_{\text{H}}(1\text{H}^{\text{o}}) = 0.2123$ $a_{\text{H}}(2\text{H}^{\text{m}}) = 0.108$ $a_{\text{H}}(1\text{H}^{\text{p}}) = 0.325$		
Toluene/2-PrOH	 , 74	$a_{\text{N}}(\text{NO}) = 1.065$ $a_{\text{H}}(\text{NOH}) = 1.114$ $a_{\text{H}}(3\text{H}^{\text{methyl}}) = 0.209$ $a_{\text{H}}(1\text{H}^{\text{o}}) = 0.209$ $a_{\text{H}}(2\text{H}^{\text{m}}) = 0.104$ $a_{\text{H}}(1\text{H}^{\text{p}}) = 0.325$		
	 , 26	$a_{\text{N}}(\text{NO}) = 0.829$ $a_{\text{H}}(3\text{H}^{\text{methyl}}) = 0.209$ $a_{\text{H}}(1\text{H}^{\text{o}}) = 0.209$ $a_{\text{H}}(2\text{H}^{\text{m}}) = 0.104$ $a_{\text{H}}(1\text{H}^{\text{p}}) = 0.322$		

^a (1:1; v/v).

the EPR spectrum corresponding to the nitroxyl $\bullet\text{ND-CH}_2\text{X}$ characterized with EPR parameters $g = 2.0056$, $a_{\text{N}}(\text{NO}) = 1.37 \text{ mT}$ and $a_{\text{H}}(2\text{H}) = 0.793 \text{ mT}$ (Fig. 7, Table 6). The analogous radical product has been observed previously during irradiation of nitrosodurene in methanol solvent [43]. Subsequently, we attribute this paramagnetic species to photoproduct of nitrosodurene direct excitation.

The series of EPR spectra measured upon continuous irradiation of nitrosodurene in toluene/MeOH (1:1 (v/v)) suspensions containing various concentrations of TiO₂ are

depicted in Fig. 8. The results obtained evidently demonstrate the significant influence of titanium dioxide concentration, as well as the effect of exposure time on the character of individual EPR spectra measured. The complex EPR spectrum measured after 12 min of continuous irradiation of ND in toluene/MeOH (1:1 (v/v)) TiO₂ suspension ($c_{\text{ND}} = 1.5 \text{ mmol dm}^{-3}$, $\rho_{\text{TiO}_2} = 1 \text{ g dm}^{-3}$) was simulated as a linear combination of three radical species (Table 6), and attributed to mono-anion $\text{ND}^{\bullet-}$, and two radical adducts $\bullet\text{ND-CH}_2\text{OH}$ and $\bullet\text{ND-CH}_2\text{X}$ in analogy with published

Table 6

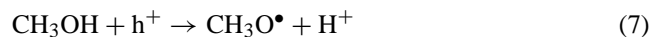
EPR parameters of radical species formed upon continuous irradiation of nitrosodurene in titanium dioxide suspensions ($c_{\text{ND}} = 1.5 \text{ mmol dm}^{-3}$)

Solvent system	TiO ₂ concentration (g dm ⁻³)	Radical, relative concentration (%)	Splitting constants (mT)	<i>g</i> -Factor	Reference
Toluene	0	•ND–CH ₂ X, 100	$a_{\text{N}}(\text{NO}) = 1.370$ $a_{\text{H}}(2\text{H}) = 0.793$	2.0057	[43]
Toluene/MeOH ^a	1.0	ND ^{-•} , 26	$a_{\text{N}}(\text{NO}) = 1.435$	2.0057	[45]
		•ND–CH ₂ OH, 53	$a_{\text{N}}(\text{NO}) = 1.435$ $a_{\text{H}}(1\text{H}) = 0.886$ $a_{\text{H}}(1\text{H}) = 0.895$ $a_{\text{N}}(\text{NO}) = 1.350$ $a_{\text{H}}(2\text{H}) = 0.790$	2.0057	[31,47]
		•ND–CH ₂ X, 21	$a_{\text{N}}(\text{NO}) = 1.390$ $a_{\text{H}}(1\text{H}) = 0.625$	2.0057	[47]
	0.1	•ND–CH(OH)CH ₃ , 69	$a_{\text{N}}(\text{NO}) = 1.440$ $a_{\text{H}}(2\text{H}) = 1.165$	2.0056	[47]
		•ND–CH ₂ CH ₂ OH, 16	$a_{\text{N}}(\text{NO}) = 1.445$ $a_{\text{H}}(3\text{H}) = 1.315$	2.0056	[47]
		•ND–CH ₃ , 11	$a_{\text{N}}(\text{NO}) = 1.435$ $a_{\text{H}}(2\text{H}) = 0.845$	2.0056	[48]
Toluene/EtOH	1.0	ND ^{-•} , 9	$a_{\text{N}}(\text{NO}) = 1.433$	2.0057	
		•ND–CH(OH)CH ₃ , 19	$a_{\text{N}}(\text{NO}) = 1.405$ $a_{\text{H}}(1\text{H}) = 0.625$	2.0057	[31]
		•ND–CH ₂ CH ₂ OH, 20	$a_{\text{N}}(\text{NO}) = 1.440$ $a_{\text{H}}(2\text{H}) = 1.158$ $a_{\text{N}}(\text{NO}) = 1.445$ $a_{\text{H}}(3\text{H}) = 1.320$		
	0.1	•ND–CH ₃ , 32	$a_{\text{N}}(\text{NO}) = 1.435$ $a_{\text{H}}(2\text{H}) = 0.845$	2.0056	[31]
		•ND–CH ₂ C ₆ H ₅ , 20	$a_{\text{N}}(\text{NO}) = 1.410$ $a_{\text{N}}(\text{NO}) = 1.410$ $a_{\text{H}}(2\text{H}) = 1.176$	2.0056	[31]
		•ND–C(OH)(CH ₃) ₂ , 41 •ND–CH ₂ CH(OH)CH ₃ , 22			
Toluene/2-PrOH	0.1	•ND–CH ₃ , 12	$a_{\text{N}}(\text{NO}) = 1.410$ $a_{\text{H}}(3\text{H}) = 1.310$ $a_{\text{N}}(\text{NO}) = 1.410$ $a_{\text{H}}(2\text{H}) = 0.820$		
		•ND–CH ₂ C ₆ H ₅ , 12	$a_{\text{N}}(\text{NO}) = 1.405$ $a_{\text{H}}(1\text{H}) = 0.570$		
		•ND–CHR ^b , 13			
	1.0	•ND–C(OH)(CH ₃) ₂ , 16.5 •ND–CH ₂ CH(OH)CH ₃ , 54	$a_{\text{N}}(\text{NO}) = 1.417$ $a_{\text{N}}(\text{NO}) = 1.420$ $a_{\text{H}}(2\text{H}) = 1.170$	2.0057	[31]
		•ND–CH ₃ , 11	$a_{\text{N}}(\text{NO}) = 1.430$ $a_{\text{H}}(3\text{H}) = 1.300$ $a_{\text{H}}(2\text{H}) = 0.830$ $a_{\text{N}}(\text{NO}) = 1.485$ $a_{\text{H}}(2\text{H}) = 0.570$		
Toluene/2-PrOH ^a	1.0	•ND–CH ₂ C ₆ H ₅ , 18			
		•ND–CHR ^b , 0.5			

^a (1:1 (v/v)).^b Unidentified adduct.

literature data [31,44]. The EPR spectrum of nitrosodurene mono-anion is characterized by hyperfine splittings $a_{\text{N}} = 1.435 \text{ mT}$, and $g = 2.0055$; these parameters are in good agreement with the EPR spectra of ND^{-•} recorded upon photochemical oxidation of [Fe(CN)₆]⁴⁻ [45].

The formation of hydroxymethyl radicals is fully compatible with photocatalytic methanol oxidation by the photogenerated TiO₂ holes (Eqs. (7) and (8)) [11,17].



The reduction potential of hydroxymethyl radicals [39] is, due to the cathodic shift in the reduction potential of nitrosodurene [32], presumably not suitable for the direct electron transfer to nitrosodurene molecule (Eq. (9)), and consequently photogenerated •CH₂OH radicals are efficiently

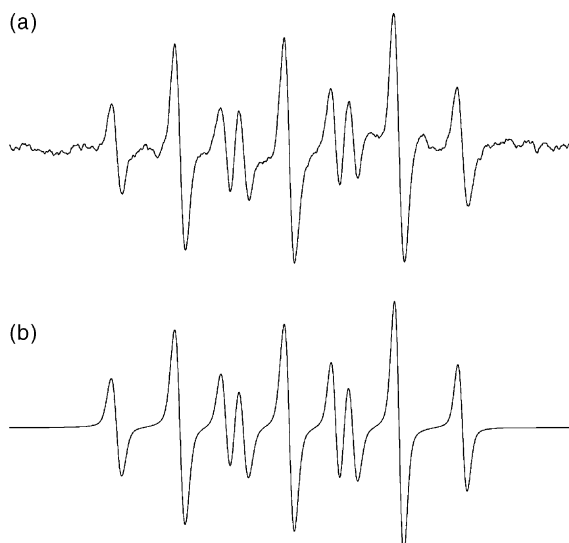
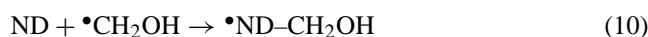


Fig. 7. Experimental (a) and simulated (b) EPR spectra (7 mT scan) obtained upon 12 min continuous irradiation of ND in toluene ($c_{\text{ND}} = 1.5 \text{ mmol dm}^{-3}$) deoxygenated by argon. The EPR parameters of simulated radical species are summarized in Table 6.

trapped, giving the characteristic nine-line EPR spectrum corresponding to the spin adduct $\bullet\text{ND}-\text{CH}_2\text{OH}$ (Eq. (10)).



The characteristics of $\bullet\text{ND}-\text{CH}_2\text{OH}$ used in the simulations of experimental spectra (Table 6) are in good accord with the reference data [31,44]. The appearance of radical adduct $\bullet\text{ND}-\text{CH}_2\text{X}$ in the experimental EPR spectra measured upon photocatalytic reduction of nitrosodurene in toluene/methanol TiO_2 suspensions reflects the contribution of direct ND photoexcitation (Table 6).

The sets of EPR spectra measured upon continuous illumination of nitrosodurene in toluene/EtOH (1:1 (v/v)) TiO_2 suspensions containing different concentrations of titanium dioxide are shown in Fig. 9. The six-line EPR spectra corresponding to $\bullet\text{ND}-\text{CH}(\text{OH})\text{CH}_3$ radical adduct dominate in the experimental spectra measured in systems with lower photocatalyst concentration ($c_{\text{ND}} = 1.5 \text{ mmol dm}^{-3}$, $\rho_{\text{TiO}_2} = 0.1 \text{ g dm}^{-3}$) and at the beginning of irradiation of systems with higher photocatalyst concentration ($c_{\text{ND}} = 1.5 \text{ mmol dm}^{-3}$, $\rho_{\text{TiO}_2} = 1.0 \text{ g dm}^{-3}$) (Fig. 9b and c).

The formation of 1-hydroxyethyl radicals is the consequence of ethanol oxidation by the titanium dioxide valence band holes (Eqs. (11) and (12)) [11,17].



However, upon prolonged irradiation the experimental EPR spectra are very complex and the simulations are based on the linear combination of four individual nitrosodurene radical adducts (Fig. 10, Table 6).

The photogenerated 1-hydroxyl radical, which represents the most stable isomer of $(\text{C}_2\text{H}_5\text{O})\bullet$ radical species, can react with ethanol molecules forming 2-hydroxyethyl radicals (Eq. (14)), which can dissociate to methyl radical and CH_2O [46] (Eq. (15)).

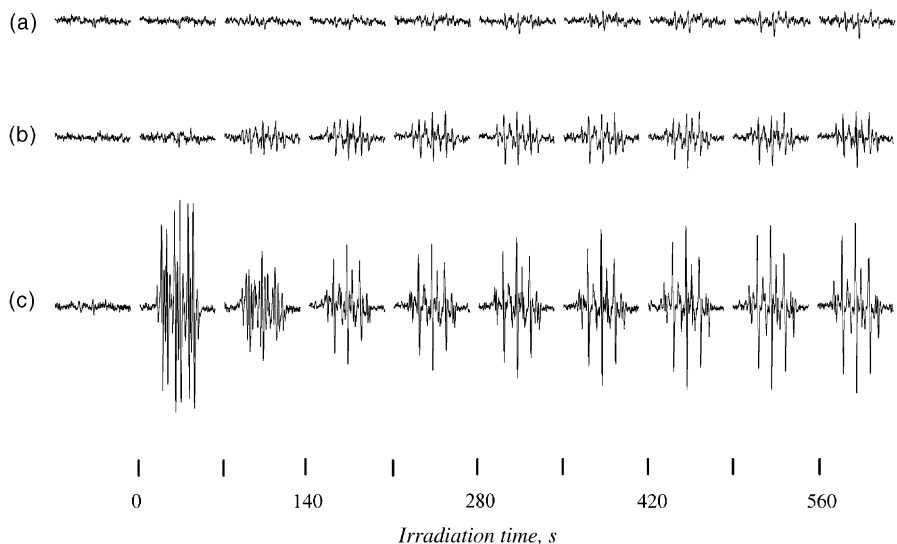
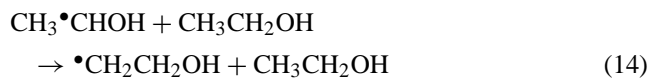


Fig. 8. Series of EPR spectra (8 mT scan) obtained upon continuous irradiation of ND in toluene/MeOH (1:1 (v/v)) TiO_2 suspensions ($c_{\text{ND}} = 1.5 \text{ mmol dm}^{-3}$) deoxygenated by argon: (a) $\rho_{\text{TiO}_2} = 0 \text{ g dm}^{-3}$; (b) $\rho_{\text{TiO}_2} = 0.1 \text{ g dm}^{-3}$; (c) $\rho_{\text{TiO}_2} = 1 \text{ g dm}^{-3}$.

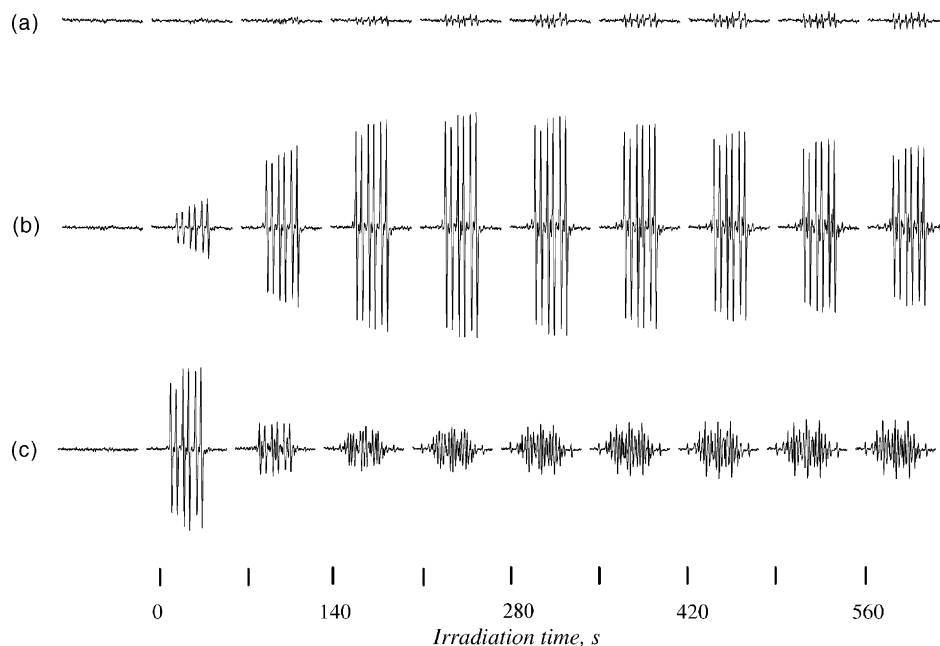


Fig. 9. Series of EPR spectra (9 mT scan) obtained upon continuous irradiation of ND in toluene/EtOH (1:1 (v/v)) TiO_2 suspensions ($c_{\text{ND}} = 1.5 \text{ mmol dm}^{-3}$) deoxygenated by argon: (a) $\rho_{\text{TiO}_2} = 0 \text{ g dm}^{-3}$; (b) $\rho_{\text{TiO}_2} = 0.1 \text{ g dm}^{-3}$; (c) $\rho_{\text{TiO}_2} = 1 \text{ g dm}^{-3}$.

The presence of 1-hydroxyethyl, 2-hydroxyethyl and methyl radical adducts is shown unambiguously by simulation of the experimental EPR spectra measured during exposure of nitrosodurene in toluene/EtOH suspensions with higher TiO_2 concentration ($c_{\text{ND}} = 1.5 \text{ mmol dm}^{-3}$, $\rho_{\text{TiO}_2} = 1 \text{ g dm}^{-3}$) (Figs. 9c and 10).

Additionally, under given experimental conditions a three-line EPR signal ascribed to nitrosodurene mono-anion is observed (Table 6), as well as the $\bullet\text{ND}-\text{CH}_2\text{C}_6\text{H}_5$ adduct corresponding to the trapped benzyl radical, which is generated by the following reactions:



The relative concentration of radical adducts corresponding to the reaction products of 1-hydroxyethyl radicals significantly increases with the concentration of titanium dioxide in the irradiated suspensions (Table 6). The adequate interpretation of experimental EPR spectra is demonstrated by good agreement of experimental and calculated EPR spectra obtained by the linear combination of individual simulations (Fig. 10).

Analogous radical processes were detected during the irradiation of nitrosodurene in toluene/2-PrOH TiO_2 suspensions with different titanium dioxide concentrations (Fig. 11). As the relative concentration of nitrosodurene mono-anion decreases with the decline of solvent permittivity we proposed that the dominating three-line EPR spectrum corresponds to the formation of radical adduct $\bullet\text{ND}-\text{C}(\text{OH})(\text{CH}_3)_2$. However, the presence of three-line

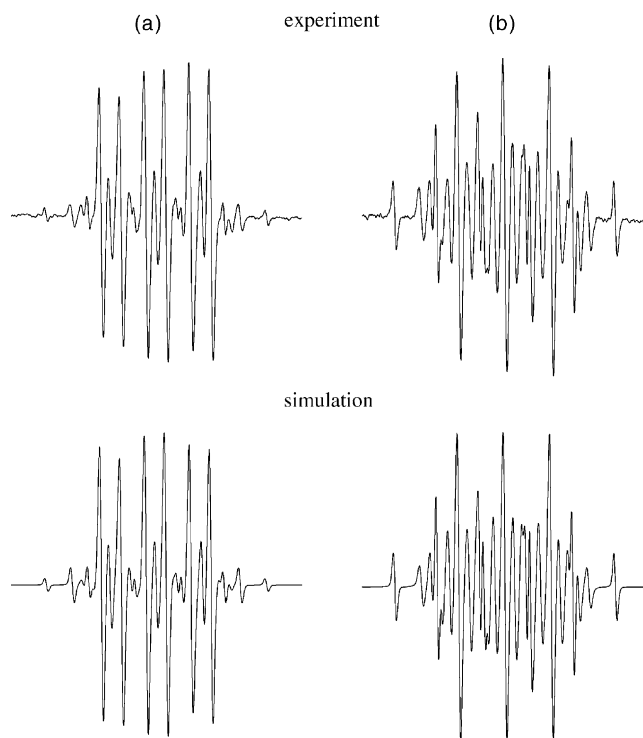


Fig. 10. Experimental and simulated EPR spectra (9 mT scan) obtained upon 12 min continuous irradiation of ND in toluene/EtOH (1:1 (v/v)) TiO_2 suspensions ($c_{\text{ND}} = 1.5 \text{ mmol dm}^{-3}$) deoxygenated by argon: (a) $\rho_{\text{TiO}_2} = 0.1 \text{ g dm}^{-3}$; (b) $\rho_{\text{TiO}_2} = 1 \text{ g dm}^{-3}$. The EPR parameters of simulated radical species are summarized in Table 6.

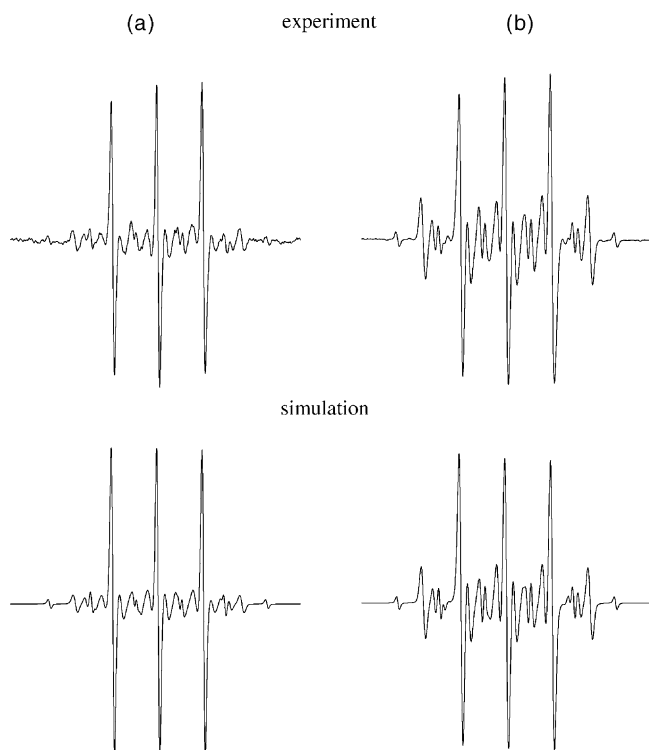
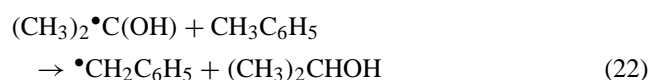
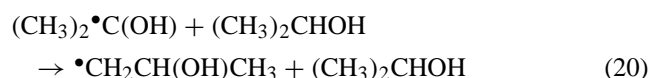
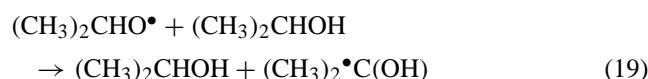
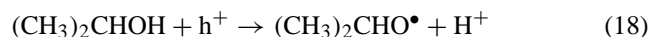


Fig. 11. Experimental and simulated EPR spectra (9 mT scan) obtained upon 12 min continuous irradiation of ND in toluene/2-PrOH (1:1 (v/v)) TiO₂ suspensions ($c_{\text{ND}} = 1.5 \text{ mmol dm}^{-3}$) deoxygenated by argon: (a) $\rho_{\text{TiO}_2} = 0.1 \text{ g dm}^{-3}$; (b) $\rho_{\text{TiO}_2} = 1 \text{ g dm}^{-3}$. The EPR parameters of simulated radical species are summarized in Table 6.

EPR signal of nitrosodurene mono-anion cannot be excluded since it can overlap the spin-adduct signal due to the similar hyperfine splittings (Table 6).

Complex EPR spectra measured upon prolonged irradiation correspond to the nitrosodurene adducts (Fig. 11, Table 6), which reflect the reaction pathways of photogenerated radical species (Eqs. (18)–(23)):



Oxygen-centered alkoxy radical species derived from an alcohol ($\text{RR}'\text{CH-O}^\bullet$) are also formed during irradiation of systems under given experimental conditions, but trapping of that type of radicals by ND is restricted due largely to poor stability of these types of adducts.

In the EPR spectra measured upon continuous irradiation of ND in toluene/alcohol (1:1 (v/v)) TiO₂ slurry (especially in initial stages of illumination), one can observe six-line EPR spectrum with hyperfine splitting constant of one hydrogen atom ($a_{\text{H}} = 0.55\text{--}0.63 \text{ mT}$), which is too low to be considered as a hydrogen directly bound to the nitrogen atom of ND. The radical species which would give such a sextet in complex EPR spectrum, might have a general formula $\bullet\text{ND}\text{-CHR}$. Those considerations are confirmed by data published in the database [31].

The relative concentration of individual radical species is significantly dependent on titanium dioxide concentration (Table 6). Fig. 11 demonstrates good harmony of experimental EPR spectra obtained after 12 min of continuous irradiation of ND in toluene/2-PrOH titanium dioxide suspensions with the simulated spectra calculated as the linear combination of five individual EPR spectra (Table 6).

3.5. Reduction of 2,4,6-tri-*t*-butyl-nitrosobenzene in titanium dioxide suspensions

The value of the (*t*-Bu)₃NOB first reduction step in acetonitrile (Fig. 1, Table 2) theoretically excludes a direct transfer of an electron from the photogenerated excited state in a titanium dioxide particle to a molecule of nitrosobenzene derivative, therefore, we expected the less effective photocatalytic reduction process to occur. However, the experimental results obtained yield unambiguous evidence that the molecule, (*t*-Bu)₃NOB, undergoes the usual electron acceptance reaction forming the corresponding reduction products, as do the other nitroso derivatives.

The irradiation of (*t*-Bu)₃NOB in toluene/methanol solvent system under given experimental conditions confirms the substantial influence of titanium dioxide concentration on the yield of photoproducted radical species. The results of blank photochemical experiments without titanium dioxide corroborate the sufficient photochemical stability of (*t*-Bu)₃NOB under given experimental conditions, as no radical products were observed when TiO₂-free solutions were irradiated. However, the irradiation of (*t*-Bu)₃NOB in toluene/methanol (1:1 (v/v)) suspensions ($c_{(\textit{t}\text{-Bu})_3\text{NOB}} = 1.5 \text{ mmol dm}^{-3}$, $\rho_{\text{TiO}_2} = 1.0 \text{ g dm}^{-3}$) leads to the efficient formation of paramagnetic species. The simulation of experimental EPR spectra measured after 12 min of continuous illumination in toluene/methanol experimental systems with different titanium dioxide concentrations illustrates Fig. 12. The simulation analysis clearly reveals the formation of two radical adducts (Table 7). The first adduct represents the nitroxyl radical (*t*-Bu)₃N[•]OB-H formed by the hydrogen abstraction and the second adduct originates by the reaction of hydroxymethyl radical with aryl nitroso derivative (Scheme 4). The relative concentration of both adducts is significantly dependent on the photocatalyst concentration in the illuminated systems (Table 7).

The EPR spectra of (*t*-Bu)₃NOB measured upon irradiation of toluene/CD₃OD (1:1 (v/v)) suspensions clearly

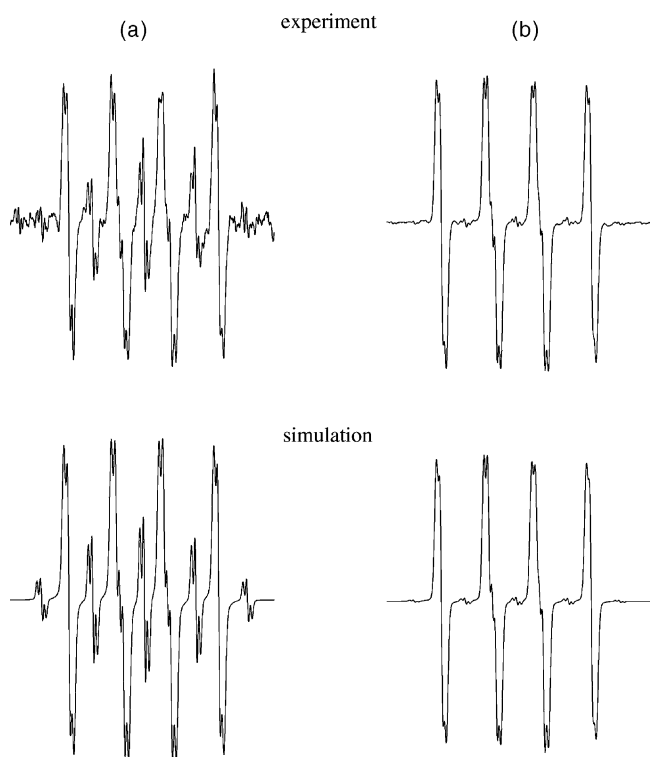


Fig. 12. Experimental and simulated EPR spectra (7 mT scan) obtained upon continuous irradiation (during 12 min) of $(t\text{-Bu})_3\text{NOB}$ in toluene/MeOH (1:1 (v/v)) TiO_2 suspensions ($c_{(t\text{-Bu})_3\text{NOB}} = 1.5 \text{ mmol dm}^{-3}$) deoxygenated by argon: (a) $\rho_{\text{TiO}_2} = 0.1 \text{ g dm}^{-3}$; (b) $\rho_{\text{TiO}_2} = 1 \text{ g dm}^{-3}$. The EPR parameters of simulated radical species are summarized in Table 7.

substantiate the efficient deuterium atom abstraction from solvent, generating the nitroxyl radical $(t\text{-Bu})_3\text{N}^*\text{OB-D}$ with typical deuterium splitting (Fig. 13).

The series of experimental EPR spectra measured upon light source exposure of $(t\text{-Bu})_3\text{NOB}$ ($c_{(t\text{-Bu})_3\text{NOB}} = 1.5 \text{ mmol dm}^{-3}$) in toluene/ethanol and toluene/2-propanol (1:1 (v/v)) suspensions with various titanium dioxide concentrations showed again the significant influence of TiO_2 photocatalyst concentration on the radical species formation. The experimental and simulated EPR spectra obtained after 12 min of continuous irradiation of $(t\text{-Bu})_3\text{NOB}$ in titanium dioxide suspensions in toluene/EtOH and toluene/2-PrOH are depicted in Fig. 14. In both solvent systems, the generation of hydrogen radical adduct $(t\text{-Bu})_3\text{N}^*\text{OB-H}$ dominates, and additionally, in toluene/ethanol the contribution of mono-anion, as well as 2-hydroxyethyl radical adduct was confirmed (Table 7). The simulation analysis of experimental spectra demonstrates unambiguously the compatibility of $(t\text{-Bu})_3\text{NOB}$ photocatalytic reduction with proposed mechanism (Scheme 1).

3.6. Reduction of 3,5-dibromo-4-nitrosobenzenesulfonate in titanium dioxide suspensions

The nitroso spin trap 3,5-dibromo-4-nitrosobenzene sulfonic acid, sodium salt (DBNBS) was developed to trap

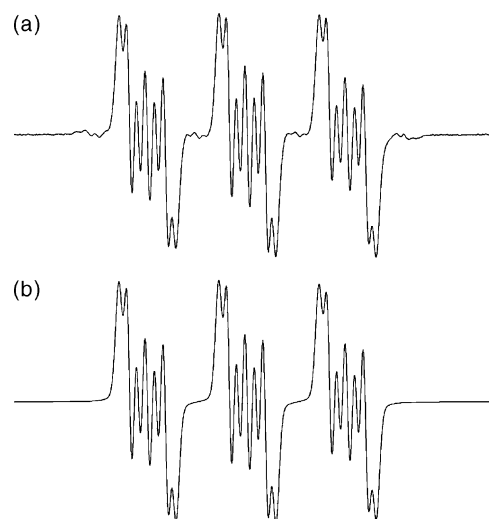


Fig. 13. Experimental (a) and simulated (b) EPR spectra (6 mT scan) obtained upon continuous irradiation of $(t\text{-Bu})_3\text{NOB}$ in toluene/ CD_3OD (1:1 (v/v)) TiO_2 suspension ($c_{(t\text{-Bu})_3\text{NOB}} = 1.5 \text{ mmol dm}^{-3}$, $\rho_{\text{TiO}_2} = 1 \text{ g dm}^{-3}$) deoxygenated by argon. The EPR parameters of simulated radical species are summarized in Table 7.

carbon-centered radicals, especially in biological systems [50–52]. This nitroso spin-trapping agent possesses good thermal and light stability [51]. In aqueous solutions DBNBS exists in a monomer/dimer equilibrium, and only

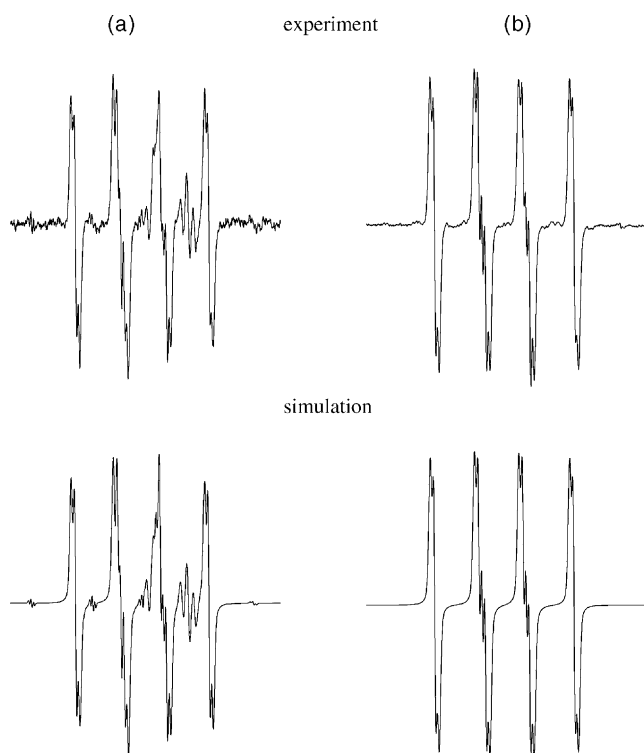
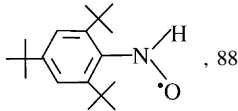


Fig. 14. Experimental and simulated EPR spectra (8 mT scan) obtained upon 12 min continuous irradiation of $(t\text{-Bu})_3\text{NOB}$ in TiO_2 suspensions ($c_{(t\text{-Bu})_3\text{NOB}} = 1.5 \text{ mmol dm}^{-3}$, $\rho_{\text{TiO}_2} = 1 \text{ g dm}^{-3}$) deoxygenated by argon: (a) toluene/EtOH (1:1 (v/v)); (b) toluene/2-PrOH (1:1 (v/v)). The EPR parameters of simulated radical species are summarized in Table 7.

Table 7

EPR parameters of radical species formed upon continuous irradiation of 2,4,6-tri-*t*-butylnitrosobenzene in titanium dioxide suspensions ($c_{(t-Bu)_3NOB} = 1.5 \text{ mmol dm}^{-3}$)

Solvent system	TiO ₂ concentration (g dm ⁻³)	Radical, relative concentration (%)	Splitting constants (mT)	<i>g</i> -Factor	Reference
	0.1	 , 88	$a_N(\text{NO}) = 1.264$ $a_H(\text{NOH}) = 1.454$ $a_H(2H^m) = 0.097$	2.0055	[49]
Toluene/CH ₃ OH ^a		(<i>t</i> -Bu) ₃ NO•B-CH ₂ R, 12	$a_N(\text{NO}) = 1.370$ $a_H(2H) = 1.363$ $a_H(2H^m) = 0.088$	2.0055	[49]
	1.0	(<i>t</i> -Bu) ₃ NO•B-H, 99	$a_N(\text{NO}) = 1.266$ $a_H(\text{NOH}) = 1.450$ $a_H(2H^m) = 0.095$		
		(<i>t</i> -Bu) ₃ NO•B-CH ₂ R, 1	$a_N(\text{NO}) = 1.367$ $a_H(2H) = 1.363$ $a_H(2H^m) = 0.088$		
Toluene/CD ₃ OD	1.0	(<i>t</i> -Bu) ₃ NO•B-D, 100	$a_N(\text{NO}) = 1.248$ $a_D(\text{NOD}) = 0.224$ $a_H(2H^m) = 0.095$		
		(<i>t</i> -Bu) ₃ NO•B-H, 87	$a_N(\text{NO}) = 1.255$ $a_H(\text{NOH}) = 1.440$ $a_H(2H^m) = 0.095$		
Toluene/EtOH	1.0	(<i>t</i> -Bu) ₃ NO•B-(CH ₂) ₂ OH, 1	$a_N(\text{NO}) = 1.470$ $a_H(2H) = 1.815$ $a_H(2H^m) = 0.070$		
		[(<i>t</i> -Bu) ₃ NOB] ^{-•} , 12	$a_N(\text{NO}) = 1.010$ $a_H(2H^m) = 0.180$		
Toluene/2-PrOH	1.0	(<i>t</i> -Bu) ₃ NO•B-H, 100	$a_N(\text{NO}) = 1.243$ $a_H(\text{NOH}) = 1.427$ $a_H(2H^m) = 0.090$		

^a (1:1 (v/v)).

the monomeric form is suitable for spin-trapping reactions [53,54]. The DBNBS monomer–dimer equilibrium constant (K_c) was determined by NMR and UV-Vis spectroscopy, and the value of $K_c = 1.3 \times 10^{-3} \text{ mol dm}^{-3}$ at 25 °C was established using both experimental techniques [53]. The introduction of a sulfonate group onto the benzene ring of nitrosobenzene derivative results in a good solubility of DBNBS in aquatic media, and on the other hand causes the insolubility in non-polar solvents, e.g. toluene. Consequently, we prepared the DBNBS stock solutions in redistilled water, and performed the photochemical and photocatalytic experiments in mixed solvents water/alcohol (1:1 (v/v)).

The information on the redox behavior of DBNBS in aquatic media is not available in literature. Gronchi et al. investigated the electrochemistry of nitroso spin trap agents in *N,N*-dimethylformamide and acetonitrile solvents [32]. They observed the significant anodic shift for the first reduction potential of 2,4,6-trichloronitrosobenzene and 2,3,4,5,6-pentafluoronitrosobenzene comparing to pristine nitrosobenzene which was explained as a consequence of strong electron-withdrawing effect of the halogen substituents [32]. Accordingly, we suggest that due to two bromine and one sulfonate substituents on the benzene moiety in DBNBS molecule, the direct transfer of TiO₂

conduction band photoelectron to nitroso group is more effective. Additionally, the 1-hydroxyalkyl radicals formed by the alcohol oxidations in titanium dioxide suspensions, may be efficiently involved in the reduction process due to the suitable potential positions [39], forming the corresponding Ar-NO•⁻ anion radical. However, the stability of photoproducted aryl-nitroso anion-radicals in protic media (water/alcohol 1:1 (v/v)) is lower compared to that in toluene/alcohol (1:1 (v/v)), and their consecutive termination reactions forming reduction products might be accelerated [32]. It is useful to note that the rate of the reaction (Ar-NHOH → Ar-NH₂) is strongly dependent on the inductive electron-withdrawing properties of ring substituents, because the electron-withdrawing nature of the substituents increases the acidity of the hydroxylamine hydrogen, increasing the electron density on the nitrogen and making the complete reduction less favorable [17]. All these phenomena decrease the probability of direct EPR observation of DBNBS anion radical, as well as its termination product formed by hydrogen abstraction from solvent surroundings formed upon irradiation under the given experimental conditions.

We observed very good photostability of DBNBS, because no paramagnetic signals were measured in the TiO₂-free methanol solutions upon irradiation of DBNBS

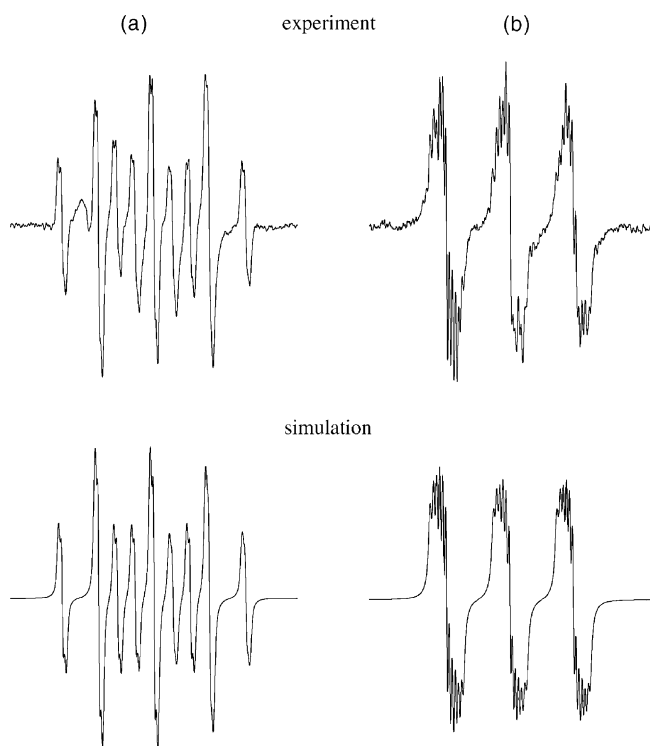


Fig. 15. Experimental and simulated EPR spectra obtained upon 12 min continuous irradiation of DBNBS in TiO_2 suspensions ($c_{\text{DBNBS}} = 1.5 \text{ mmol dm}^{-3}$, $\rho_{\text{TiO}_2} = 1 \text{ g dm}^{-3}$) deoxygenated by argon: (a) $\text{H}_2\text{O}/\text{MeOH}$ (1:1 (v/v)), 7 mT scan; (b) $\text{H}_2\text{O}/\text{CD}_3\text{OD}$ (1:1 (v/v)), 6 mT scan. The EPR parameters of simulated radical species are summarized in Table 8.

under given irradiation conditions. The analogous status is also found when methanol is replaced by ethanol or 2-propanol. Additionally, only negligible EPR intensity of radical products is observed, when DBNBS is irradiated in water/methanol system with lower TiO_2 concentration ($\rho_{\text{TiO}_2} = 0.1 \text{ g dm}^{-3}$). However, the increase of photocatalyst concentration in the investigated system ($\rho_{\text{TiO}_2} = 1 \text{ g dm}^{-3}$) leads to the generation of $\bullet\text{CH}_2\text{OH}$ radical, which is identified as corresponding DBNBS spin adduct (Fig. 15 and Table 8). The oxidation of methanol to hydroxymethyl radicals during the photocatalytic redox process in the presence of DBNBS is confirmed by the application of deuterated methanol. Under these experimental conditions, the $\bullet\text{DBNBS-CD}_2\text{OD}$ radical adduct is detected and monitored (Fig. 15).

Fig. 16 shows the results of photochemical experiments carried with DBNBS ($c_{\text{DBNBS}} = 1.5 \text{ mmol dm}^{-3}$) in water/ethanol and water/2-propanol (1:1 (v/v)) solutions with TiO_2 suspensions. The simulation analysis of experimental EPR spectra obtained after 12 min of irradiation DBNBS in water/ethanol TiO_2 suspensions clearly showed the presence of two radical adducts corresponding to the addition of $\bullet\text{CH}_2\text{CH}_2\text{OH}$ and $\bullet\text{CH}_3$ radicals to the nitroso group. The primary photogenerated 1-hydroxyethyl radical is not observed (Fig. 16a), which is in a good correlation with the

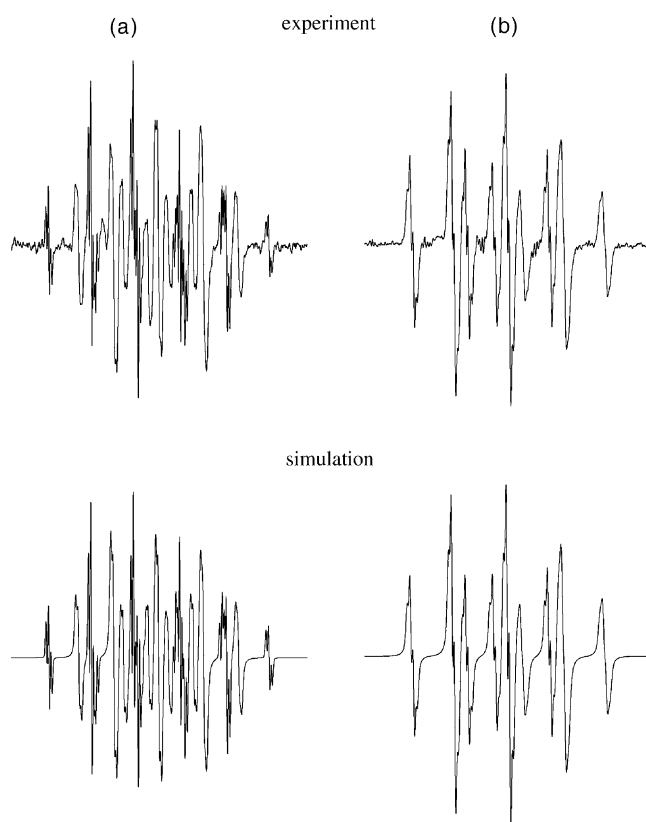


Fig. 16. Experimental and simulated EPR spectra obtained upon 12 min continuous irradiation of DBNBS in TiO_2 suspensions ($c_{\text{DBNBS}} = 1.5 \text{ mmol dm}^{-3}$, $\rho_{\text{TiO}_2} = 1 \text{ g dm}^{-3}$) deoxygenated by argon: (a) $\text{H}_2\text{O}/\text{EtOH}$ (1:1 (v/v)), 9 mT scan; (b) $\text{H}_2\text{O}/2\text{-PrOH}$ (1:1 (v/v)), 7 mT scan. The EPR parameters of simulated radical species are summarized in Table 8.

previously mentioned tentative predictions assuming rapid reduction of DBNBS. The analogous situation occurs in the irradiated water/2-propanol titanium dioxide suspensions, as here the simulation of experimental EPR spectra reveals exclusively the formation of $\bullet\text{DBNBS-CH}_2\text{CH}(\text{OH})\text{CH}_3$ radical adduct (Fig. 16b). It should be noted here, that the satisfactory simulation of experimental EPR spectra corresponding to DBNBS adducts requires the incorporation of a tumbling effect in the calculation procedure.

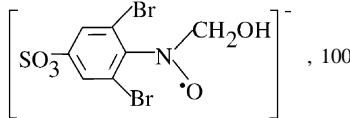
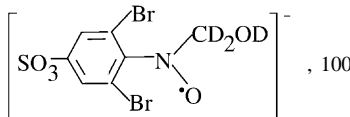
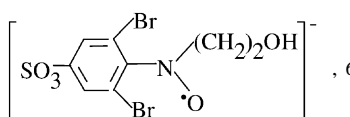
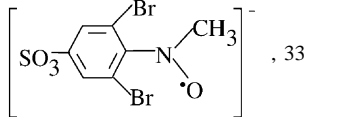
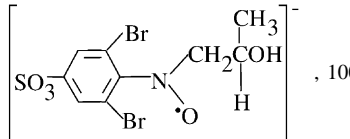
3.7. Reduction of 2-methyl-2-nitrosopropane in titanium dioxide suspensions

The extensively applied spin-trapping agent 2-methyl-2-nitrosopropane (MNP) has been shown to be suitable, especially for carbon-centered radicals identification [31]. However, it easily decomposes thermally and photochemically, producing the stable radical adduct di-*t*-butylnitroxide (Scheme 5).

The di-*t*-butylnitroxide radical is characterized by a triplet EPR spectrum arising from nitrogen hyperfine splitting; in literature the value of $a_{\text{N}} \sim 1.6 \text{ mT}$ is reported [57–59]. The molecule of MNP is photosensitive in the wavelength

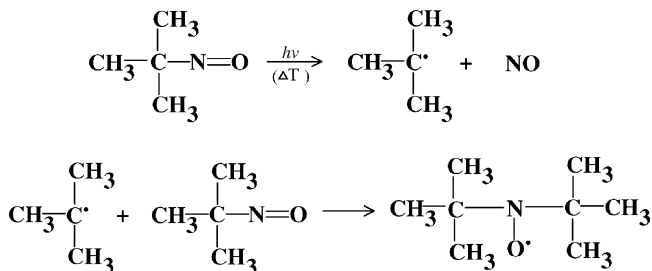
Table 8

EPR parameters of radical species formed upon continuous irradiation of 3,5-dibromo-4-nitrosobenzene sulfonate in titanium dioxide suspensions ($c_{\text{DBNBS}} = 1.5 \text{ mmol dm}^{-3}$, $\rho_{\text{TiO}_2} = 1.0 \text{ g dm}^{-3}$)

Solvent system	Radical, relative concentration (%)	Splitting constants (mT)	<i>g</i> -Factor	Reference
H ₂ O/CH ₃ OH ^a	 , 100	$a_{\text{N}}(\text{NO}) = 1.350$ $a_{\text{H}}(2\text{H}) = 0.890$ $a_{\text{H}}(2\text{H}^m) = 0.067$	2.0060	[55]
H ₂ O/CD ₃ OD	 , 100	$a_{\text{N}}(\text{NO}) = 1.355$ $a_{\text{H}}(2\text{D}) = 0.139$ $a_{\text{H}}(2\text{H}^m) = 0.070$		
H ₂ O/EtOH	 , 67	$a_{\text{N}}(\text{NO}) = 1.365$ $a_{\text{H}}(2\text{H}) = 1.064$ $a_{\text{H}}(2\text{H}^m) = 0.067$	2.0060	[55]
	 , 33	$a_{\text{N}}(\text{NO}) = 1.410$ $a_{\text{H}}(3\text{H}) = 1.290$ $a_{\text{H}}(2\text{H}^m) = 0.070$	2.0060	[50,54]
H ₂ O/2-PrOH	 , 100	$a_{\text{N}}(\text{NO}) = 1.340$ $a_{\text{H}}(2\text{H}) = 1.003$ $a_{\text{H}}(1\text{H}) = 0.070$ $a_{\text{H}}(2\text{H}^m) = 0.065$	2.0060	[56]

^a (1:1 (v/v)).

range between 320–360 nm and 660–680 nm. Leastic et al. [59] performed the photocatalytic EPR experiments in the irradiated WO₃ suspensions applying only the selected wavelength of 390 nm in order to avoid the formation of di-*t*-butylnitroxide adduct. However, the EPR spectra measured by the monochromatic excitation ($\lambda = 390 \text{ nm}$) of aqueous WO₃ suspensions in the presence of ethanol or acetone resulted in the formation of $\bullet\text{CH}(\text{OH})\text{CH}_3$ or $\bullet\text{CH}_2\text{COCH}_3$ adducts characterized by very low intensities. In our photocatalytic experiments, the utilization of titanium dioxide photocatalyst requires the excitation wavelengths <400 nm, and we use no optical filter for the suitable wavelength selection.



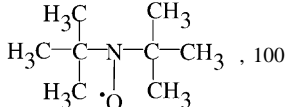
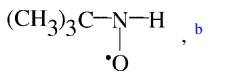
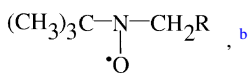
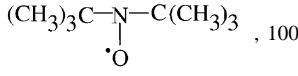
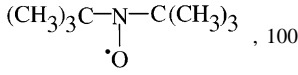
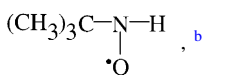
Scheme 5. Photochemical or thermal decomposition of MNP and consecutive di-*t*-butylnitroxide radical adduct formation.

The triplet EPR signal ($a_{\text{N}} = 1.623 \text{ mT}$, $g = 2.0055$) represents the characteristic feature of the EPR spectra monitored upon irradiation of MNP in toluene/methanol solutions (1:1 (v/v); $c_{\text{MNP}} = 1.5 \text{ mmol dm}^{-3}$) without titanium dioxide. This high-intensity EPR signal, which corresponds to the abovementioned di-*t*-butylnitroxide radical, is produced by an effective MNP photoexcitation. The EPR spectra, which were of good quality enabled us to resolve the hyperfine splittings of ¹³C satellites in addition to those of the nitrogen atom (Table 9). The presence of titanium dioxide in the experimental systems has only a negligible influence on the character of the EPR spectra, since most likely, the dominant part of the irradiation is absorbed by MNP molecules. It does, however affect the intensity of individual EPR spectra monitored during irradiation. The detailed analysis of the experimental spectra measured in MNP toluene/methanol (1:1 (v/v)) TiO₂ suspensions ($c_{\text{MNP}} = 1.5 \text{ mmol dm}^{-3}$, $\rho_{\text{TiO}_2} = 1 \text{ g dm}^{-3}$) reveals the presence of low concentration (the relative concentration is lower than 0.1 %) of MNP radical adducts corresponding to the addition of hydrogen and hydroxymethyl radical (Fig. 17, Table 9).

The predominating EPR signal monitored upon the photoexcitation of MNP ($c_{\text{MNP}} = 1.5 \text{ mmol dm}^{-3}$) in toluene/ethanol mixed solvent (1:1 (v/v)) in the absence, as well as in the presence of titanium dioxide photocatalyst

Table 9

EPR parameters of radical species formed upon continuous irradiation of 2-methyl-2-nitrosopropane in titanium dioxide suspensions ($c_{\text{MNP}} = 1.5 \text{ mmol dm}^{-3}$, $\rho_{\text{TiO}_2} = 1.0 \text{ g dm}^{-3}$)

Solvent system	Radical, relative concentration (%)	Splitting constants (mT)	<i>g</i> -Factor	Reference
Toluene/CH ₃ OH ^a	 , 100	$a_{\text{N}}(\text{NO}) = 1.623$ $a_{13\text{C}}(2^{13}\text{C}) = 0.480$ $a_{13\text{C}}(6^{13}\text{C}) = 0.450$	2.0055	[57–59]
	 , ^b	$a_{\text{N}}(\text{NO}) = 1.377$ $a_{\text{H}}(\text{NOH}) = 1.255$	2.0056	[31,60]
	 , ^b	$a_{\text{N}}(\text{NO}) = 1.140$ $a_{\text{H}}(2\text{H}) = 1.273$	2.0055	[31,60]
Toluene/EtOH	 , 100	$a_{\text{N}}(\text{NO}) = 1.613$ $a_{13\text{C}}(2^{13}\text{C}) = 0.480$ $a_{13\text{C}}(6^{13}\text{C}) = 0.440$		
Toluene/2-PrOH	 , 100	$a_{\text{N}}(\text{NO}) = 1.600$ $a_{13\text{C}}(2^{13}\text{C}) = 0.480$ $a_{13\text{C}}(6^{13}\text{C}) = 0.440$		
	 , ^b	$a_{\text{N}}(\text{NO}) = 1.367$ $a_{\text{H}}(\text{NOH}) = 1.234$		

^a (1:1 (v/v)).

^b Negligible contribution.

corresponds again to the di-*t*-butylnitroxide radical formation. The simulation analysis shows very good agreement of the calculated simulation and experimental EPR spectra (Table 9).

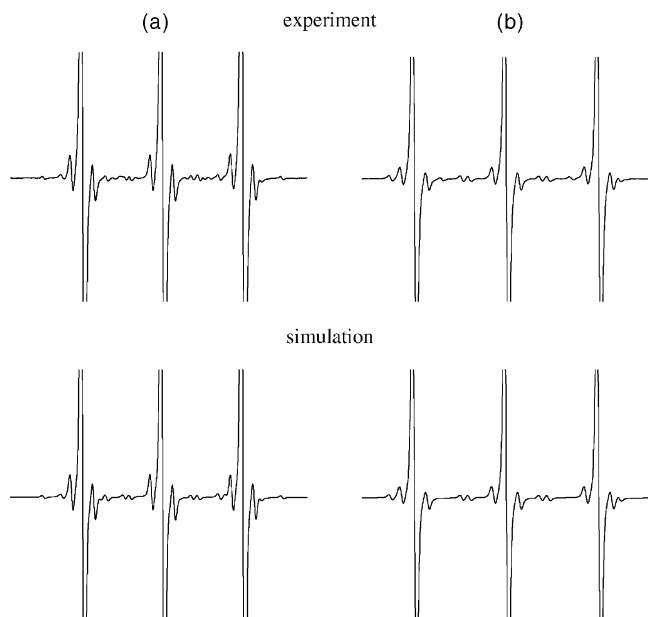


Fig. 17. Experimental and simulated EPR spectra (6 mT scan) obtained upon 12 min continuous irradiation of MNP in TiO₂ suspensions ($c_{\text{MNP}} = 1.5 \text{ mmol dm}^{-3}$, $\rho_{\text{TiO}_2} = 1 \text{ g dm}^{-3}$) deoxygenated by argon: (a) toluene/MeOH (1:1 (v/v)); (b) toluene/2-PrOH (1:1 (v/v)). The spectra are delineated in higher gain to appear signals with lower intensity. The EPR parameters of simulated radical species are summarized in Table 9.

The photostability of MNP in the solvent system toluene/2-propanol (1:1 (v/v)) is very low, since the typical nitrogen triplet splitting can readily be observed after manipulation with an EPR flat cell in the laboratory without in situ excitation in the EPR spectrometer cavity. The EPR spectra measured in toluene/2-propanol photochemical and photocatalytic experimental systems disclose the formation of the di-*t*-butylnitroxide radical. However, careful examination of the EPR spectra monitored in TiO₂ suspensions reveals very low contribution of the (CH₃)₃CN•OH radical (Fig. 17, Table 9).

4. Conclusions

The photocatalytic reduction of nitroso compounds (nitrosobenzene, 2-nitrosotoluene, 2,3,5,6-tetramethylnitrosobenzene (nitrosodurene), 2,4,6-tri-*t*-butylnitrosobenzene, 3,5-dibromo-4-nitroso-benzenesulfonate, 2-methyl-2-nitrosopropane) was investigated in the irradiated titanium dioxide suspensions prepared in mixed solvents toluene/alcohol or water/alcohol for in situ EPR spectroscopy. The results obtained may be summarized as follows:

- The position of titanium dioxide conduction band-edge along with the nitroso compounds first reduction step potentials in studied systems, predetermines the character of radical species monitored upon continuous irradiation. The photoinduced electron transfer from TiO₂ to nitroso compounds is accompanied by alcohol oxidation via the photogenerated titanium dioxide valance band

holes forming primary hydroxyalkyl radicals ($\bullet\text{CH}_2\text{OH}$, $\bullet\text{CH}(\text{OH})\text{CH}_3$, $\bullet\text{C}(\text{OH})(\text{CH}_3)_2$). Production of hydroxyalkyl radicals with redox potentials suitable for a direct electron transfer to nitroso compounds represents an alternative reaction pathway for their reduction. On the other hand, since the investigated nitroso derivatives are efficient spin-trapping agents, the formation of their nitroxyl radical adducts was observed in the photocatalytic experiments.

- Nitrosobenzene is efficiently reduced in the irradiated TiO_2 suspensions (toluene/alcohol, 1:1; v/v) forming exclusively one stable radical intermediate corresponding to $\text{C}_6\text{H}_5\text{N}^\bullet\text{OH}$ species. The formation of this radical species is consistent with the proposed mechanism (Scheme 2), occurring from the primary generated nitrosobenzene mono-anion by the hydrogen abstraction from surroundings. The origin of hydrogen added to the nitroso group was determined by the photocatalytic experiments using deuterated methanol, where the production of $\text{C}_6\text{H}_5\text{N}^\bullet\text{OD}$ was confirmed. Additionally, an identical radical was detected, when nitrobenzene was reduced under analogous experimental conditions.
- The photocatalytic reduction of 2-nitrosotoluene in TiO_2 suspensions resulted in complex EPR spectra, due to radicals formed when hydrogen addition to the nitroso group occurred forming the $\text{CH}_3\text{C}_6\text{H}_4\text{N}^\bullet\text{OH}$ adduct; the other observed radical species was attributed to 2-nitrosotoluene mono-anion. However, a further improvement of experimental spectra simulation required the incorporation of additional radical structures, such as hydroxyalkyl radical adducts.
- Nitrosodurene revealed significant photosensitivity under the given experimental conditions, when even the irradiation of the TiO_2 -free systems led also to the formation of radical adducts. As the presence of tetramethyl substitution caused a significant cathodic shift of the first reduction step potential, the formation of nitrosodurene reduction products by electron transfer was partially hindered, and the signals corresponding to the addition of hydroxyalkyl radicals or their consecutive products, predominated in the experimental EPR spectra.
- The energy levels of 2,4,6-tri-*t*-butylnitrosobenzene molecules are suitably positioned for a direct transfer of photogenerated electrons, hence hydrogen adduct (*t*-Bu) $_3\text{C}_6\text{H}_2\text{N}^\bullet\text{OH}$ dominated the experimental spectra.
- The spin-trapping agent 3,5-dibromo-4-nitroso-benzene-sulfonate was, due to its insolubility in toluene irradiated in titanium dioxide suspensions prepared in water/alcohol mixtures. EPR spectra measured under these experimental conditions represented the spin adducts of the hydroxyalkyl radicals or their consecutive products.
- The photochemical behavior of 2-methyl-2-nitrosopropane was quite different comparing to aryl nitroso derivatives, because this nitroso compound is extremely photosensitive under given experimental condition, and also the position of titanium dioxide conduction band-edge along

with the MNP first reduction step potential is unsuitable for photoinduced electron transfer under the given experimental conditions. The irradiation caused a significant yield of di-*t*-butylnitroxide, and the formation or addition of further radical species was, in fact, negligible.

Acknowledgements

We thank Slovak Grant Agency for the financial support (Project VEGA/1/7313/20). Dr. Vladimír Mišík is gratefully acknowledged for the helpful discussion, and the referee for the valuable comments.

References

- [1] A. Fujishima, K. Honda, *Nature* 37 (1972) 238.
- [2] M. Grätzel (Ed.), *Resources Through Photochemistry and Catalysis*, Academic Press, New York, 1983.
- [3] N. Vlachopoulos, P. Liska, J. Augustynski, M. Grätzel, *J. Am. Chem. Soc.* 110 (1988) 1216.
- [4] P.V. Kamat, N.M. Dimitrijevic, *Solar Energy* 44 (1990) 83.
- [5] N. Serpone, in: J.R. Norris, D. Meisel (Eds.), *Photochemical Energy Conversion*, Elsevier, Amsterdam, The Netherlands, 1989, p. 297.
- [6] M. Grätzel, in: E. Pelizzetti, N. Serpone (Eds.), *Homogeneous and Heterogeneous Photocatalysis*, D. Reidel Publishing Company, Dordrecht, The Netherlands, 1986, p. 91.
- [7] M.R. Hoffmann, S.T. Martin, W. Choi, D.W. Bahnemann, *Chem. Rev.* 95 (1995) 69.
- [8] O. Legrini, E. Oliveros, A.M. Braun, *Chem. Rev.* 93 (1993) 671.
- [9] A. Mills, R.H. Davies, D. Worsley, *Chem. Soc. Rev.* 22 (1993) 417.
- [10] R. Benedix, F. Dehn, J. Quaas, M. Orgass, *Lacer* (2000) 157. <http://www.uni-leipzig.de/~massivb/institut/lacer/lacer05/>.
- [11] Y. Li, L. Wang, in: P.V. Kamat, D. Meisel (Eds.), *Semiconductor Nanoclusters* (Studies in Sur. Sci. Cat. 103), Elsevier, Amsterdam, The Netherlands, 1996.
- [12] M.A. Fox, in: N. Serpone, E. Pelizzetti (Eds.), *Photocatalysis: Fundamental and Applications*, Wiley, New York, 1989, p. 420.
- [13] H. Al-Ekabi, in: V. Ramamurthy (Ed.), *Photochemistry in Organized and Constrained Media*, VCH, New York, 1991, p. 495.
- [14] M.A. Fox, *Top. Curr. Chem.* 142 (1991) 71.
- [15] M.A. Fox, M.T. Dulay, *Chem. Rev.* 93 (1993) 341.
- [16] F. Mahdavi, T.C. Bruton, Y. Li, *J. Org. Chem.* 58 (1993) 744.
- [17] J.L. Ferry, W.H. Glaze, *Langmuir* 14 (1998) 3551.
- [18] C.D. Jaeger, A.J. Bard, *J. Phys. Chem.* 83 (1979) 3146.
- [19] M.J. Bahneman, J. Moenig, R. Chapman, *J. Phys. Chem.* 91 (1987) 3782.
- [20] W. Choi, M.R. Hoffmann, *Environ. Sci. Technol.* 27 (1995) 1646.
- [21] W.H. Glaze, J.F. Kenneke, J.L. Ferry, *Environ. Sci. Technol.* 27 (1993) 177.
- [22] J.F. Kenneke, J.L. Ferry, W.H. Glaze, in: D.F. Ollis, H. Al-Ekabi (Eds.), *Photocatalytic Purification and Treatment of Water and Air*, Elsevier, Amsterdam, The Netherlands, 1993.
- [23] D. Duonghong, J. Ramsden, M. Grätzel, *J. Am. Chem. Soc.* 104 (1982) 2977.
- [24] V. Brezová, A. Blažková, I. Šurina, B. Havlínová, *J. Photochem. Photobiol. A: Chem.* 107 (1997) 233.
- [25] L.J. Núñez-Vergara, J.A. Squella, C. Olea-Azar, S. Bollo, P.A. Navarrete-Encina, J.C. Sturm, *Electrochem. Acta* 45 (2000) 3555.
- [26] L.J. Núñez-Vergara, M. Bontá, J.C. Sturm, P.A. Navarrete-Encina, S. Bollo, J.A. Squella, *Electroanal. Chem.* 506 (2001) 48.
- [27] S. Fadlallah, S.F. Cooper, G. Perrault, G. Truchon, J. Lesage, *Bull. Environ. Contam. Toxicol.* 57 (1996) 867.

- [28] R.F. Haseloff, K. Mertsch, E. Rohde, I. Baeger, I.A. Grigoriev, I.E. Blasig, *FEBS Lett.* 418 (1997) 73.
- [29] J. Barek, J. Cvačka, A. Muck, V. Quaserová, J. Zima, *Fresenius J. Anal. Chem.* 369 (2001) 556.
- [30] A. Staško, V. Brezová, S. Biskupič, K. Ondriaš, V. Mišík, *Free Rad. Biol. Med.* 17 (1994) 545.
- [31] A.S.W. Li, K.B. Cummings, H.P. Roethling, G.R. Buettner, C.F. Chignell, *J. Magn. Reson.* 79 (1988) 140, <http://epr.niehs.nih.gov>.
- [32] G. Gronchi, P. Courbis, P. Tordo, G. Mousset, J. Simonet, *J. Phys. Chem.* 87 (1983) 1343.
- [33] V. Cerri, C. Frejaville, F. Vila, A. Allouche, G. Gronchi, P. Tordo, *J. Org. Chem.* 54 (1989) 1447.
- [34] G. Gronchi, P. Tordo, *Res. Chem. Intermed.* 19 (1993) 733.
- [35] Catalogue of Light Sources 2000–2002, Philips Inc. <http://www.philips.com>.
- [36] R.T. Weber, Win-EPR SimFonia Manual, EPR Division, Bruker Instruments Inc., Billerica, MA, USA.
- [37] B.A. Kraeutler, A.J. Bard, *J. Am. Chem. Soc.* 100 (1978) 5985.
- [38] R.C. Larson, R.T. Iwamoto, R.N. Adams, *Anal. Chim. Acta* 25 (1961) 371.
- [39] K.-D. Asmus, G. Beck, A. Henglein, A. Wigger, *Ber. Bunsenges. Phys. Chem.* 70 (1966) 869.
- [40] http://www.chm.bris.ac.uk/emr/conferences/Pd/spectra/sim_nbh.gif.
- [41] Landolt-Börnstein, in: H. Fischer (Ed.), *Numerical Data and Functional Relationships in Science and Technology, New Series, vol. 17, Magnetic Properties of Free Radicals, Subvolume d1, Nitroxide Radicals Part 1*, Springer, Berlin, 1989, p. 212.
- [42] M. Witanowski, Z. Biedrzycka, W. Sicinska, G.A. Webb, *Magn. Reson. Chem.* 35 (1997) 262.
- [43] J. Šima, V. Brezová, *Monatsheft. Chem.* 132 (2001) 1493.
- [44] A. Staško, K. Erentová, P. Rapta, O. Nuyken, B. Voit, *Magn. Reson. Chem.* 36 (1998) 13.
- [45] D. Rehorek, *Z. Chem.* 20 (1980) 30.
- [46] M. Choi, R.T. Bise, D.M. Neumark, *J. Phys. Chem.* 104 (2000) 10112.
- [47] Landolt-Börnstein, in: H. Fischer (Ed.), *Numerical Data and Functional Relationships in Science and Technology, New Series, vol. 17, Magnetic Properties of Free Radicals, Subvolume d1, Nitroxide Radicals Part 1*, Springer, Berlin, 1989, p. 269.
- [48] J. Šima, D. Lauková, V. Brezová, *Coll. Czech. Chem. Commun.* 66 (2001) 109.
- [49] Landolt-Börnstein, in: H. Fischer (Ed.), *Numerical Data and Functional Relationships in Science and Technology, New Series, vol. 17, Magnetic Properties of Free Radicals, Subvolume d1, Nitroxide Radicals Part 1*, Springer, Berlin, 1989, p. 328.
- [50] V. Mišík, P. Riesz, *Free Rad. Biol. Med.* 26 (1999) 936.
- [51] A. Filosa, A.M. English, *J. Biol. Chem.* 276 (2001) 21022.
- [52] T. Konovalova, L.D. Kispert, N.E. Polyakov, T.V. Leshina, *Free Rad. Biol. Med.* 28 (2002) 1030.
- [53] H. Ide, A. Hagi, S. Ohsumi, A. Murakami, K. Makino, *Biochem. Int.* 27 (1992) 367.
- [54] V. Mišík, L.J. Kirschenbaum, P. Riesz, *J. Phys. Chem.* 99 (1995) 5970.
- [55] Landolt-Börnstein, in: H. Fischer (Ed.), *Numerical Data and Functional Relationships in Science and Technology, New Series, vol. 17, Magnetic Properties of Free Radicals, Subvolume d1, Nitroxide Radicals Part 1*, Springer, Berlin, 1989, p. 256.
- [56] Landolt-Börnstein, in: H. Fischer (Ed.), *Numerical Data and Functional Relationships in Science and Technology, New Series, vol. 17, Magnetic Properties of Free Radicals, Subvolume d1, Nitroxide Radicals Part 1*, Springer, Berlin, 1989, p. 257.
- [57] Y. Li, Q. Wang, J. Guo, G. Wu, *Mat. Sci. Eng. C* 10 (1999) 25.
- [58] M.M. Castellanos, D. Reyman, C. Sieiro, P. Calle, *Ultrason. Sonochem.* 8 (2001) 17.
- [59] A. Leastic, F. Babonneau, J. Livage, *J. Phys. Chem.* 90 (1986) 4196.
- [60] Landolt-Börnstein, in: H. Fischer (Ed.), *Numerical Data and Functional Relationships in Science and Technology, New Series, vol. 17, Magnetic Properties of Free Radicals, Subvolume d1, Nitroxide Radicals Part 1*, Springer, Berlin, 1989, p. 111.